Geochemistry Geophysics Geosystems G3

Article
Volume 14, Number 7
29 July 2013
doi: 10.1002/ggge.20151
ISSN: 1525-2027

Published by AGU and the Geochemical Society

The 1874–1876 volcano-tectonic episode at Askja, North Iceland: Lateral flow revisited

Margaret E. Hartley
School of GeoSciences, University of Edinburgh, Grant Institute, Edinburgh, UK

Department of Earth Sciences, University of Cambridge, Downing Street, Cambridge, CB2 3EQ, UK (meh43@cam.ac.uk)

Thor Thordarson
School of GeoSciences, University of Edinburgh, Grant Institute, Edinburgh, UK

Institute of Earth Sciences, University of Iceland, Reykjavík, Iceland

[1] The Askja volcanic system, North Iceland, experienced a volcano-tectonic episode between 1874 and 1876, the climax of which was a rhyolitic, phreatoplinian to Plinian eruption at Askja central volcano on 28–29 March 1875. Fissure eruptions also occurred in 1875, producing the Nýjahraun lava, 45–65 km north of Askja. The Nýjahraun basalt is indistinguishable, in terms of whole-rock major elements, from the small-volume basaltic eruptions that took place at Askja in the early 20th century. It has been suggested that all of these basalts originated from a shallow magma chamber beneath Askja, with the Nýjahraun eruptions being fed by northward-propagating lateral dykes. It has also been conjectured that the Holuhraun lava, located at the southern tip of the Askja volcanic system 15–25 km south of Askja, was connected with the 1874–1876 Askja volcano-tectonic episode. We re-examine these interpretations in light of new whole-rock, glass and melt inclusion analyses from samples collected along the length of the Askja volcanic system. Glasses from Nýjahraun and the Askja 20th century eruptions are geochemically distinct. We suggest that the Askja 20th century basalts mixed with evolved melts in the crust, while the Nýjahraun magma evolved without such interactions. The Holuhraun basalt is more similar to lavas erupted on the Bárðarbunga-Veiðivötn volcanic system than to postglacial basalts from Askja, indicating that particular geochemical signatures are not necessarily confined to the tectonic or structural surface expression of single volcanic systems. This has important implications for the identification and delineation of individual volcanic systems beneath the northwest sector of Vatnajökull.

Components: 14,120 words, 13 figures, 1 table.

Keywords: Iceland; lateral flow; melt transport; volcanic systems.

Index Terms: 1065 Major and trace element geochemistry: Geochemistry; 1032 Mid-oceanic ridge processes: Geochemistry; 1043 Fluid and melt inclusion geochemistry: Geochemistry; 1090 Field relationships: Geochemistry; 8416 Mid-oceanic ridge processes: Volcanology; 8486 Field relationships: Volcanology; 3640 Igneous petrology: Mineralogy and Petrology; 3614 Mid-oceanic ridge processes: Mineralogy and Petrology; 3690 Field relationships: Mineralogy and Petrology.

Received 29 January 2013; **Revised** 8 April 2013; **Accepted** 14 April 2013; **Published** 29 July 2013.

Hartley, M. E., and T. Thordarson (2013), The 1874–1876 volcano-tectonic episode at Askja, North Iceland: Lateral flow revisited, *Geochem. Geophys. Geosyst., 14*, 2286–2309, doi:10.1002/ggge.20151.

1. Introduction

[2] The volcanic system may be viewed as the principal geological structure in Iceland, and defines a characteristic volcano-tectonic architecture featuring a fissure or dyke swarm and/or a central volcano [*Bárðarson*, 1929; *Einarsson and Sæmundsson*, 1987; *Thordarson and Larsen*, 2007, and references therein]. Fissure swarms are typically elongate structures aligned parallel or subparallel to the spreading axis of the hosting volcanic system, while the central volcano (where present) is the focal point of eruptive activity. Debate on Icelandic volcano-tectonic episodes that simultaneously activate the central volcano and the surrounding fissure swarm centres on two contrasting ideas (Figure 1). According to the lateral flow hypothesis, replenishment and pressurization of a shallow magma chamber beneath a central volcano causes the lateral injection of shallow crustal dykes into the fissure swarm [e.g., *Sigurðsson and Sparks*, 1978a]. The injection of lateral dykes is thus viewed as the driving mechanism of rifting on the volcanic system. By contrast, the magma reservoir hypothesis suggests that volcano-tectonic episodes are driven by magma pressurization in large, elongate reservoirs at the base of the crust (>20 km depth) and subsequent injection of subvertical dykes into the crust [e.g., *Gudmundsson*, 1995].

[3] The Askja volcanic system, North Iceland (Figure 2a), provides a natural laboratory for investigating the mechanisms of melt generation and transport in Icelandic volcanic systems. Askja central volcano and fissure swarm were simultaneously active during a volcano-tectonic episode that began with seismicity in late 1874 and lasted until early 1876 [e.g., *Gunnarsson*, 1875; *Guðmundsson*, 1932; *Jónsson*, 1945; *Sigurðsson and Sparks*, 1978a; *Brandsdóttir*, 1992]. On the Askja fissure swarm, a basaltic fissure eruption occurred at the Sveinagjá graben, 45–60 km north of Askja, producing the Nýjahraun lava in at least six eruptive episodes between February and October 1875 (Figure 2b). At Askja central volcano, precursory phreatic, phreatomagmatic and magmatic activity culminated in an explosive, Plinian eruption on 28–29 March 1875, during which rhyolitic tephra was deposited around the Askja region and transported as far as Sweden and Norway by prevailing westerly winds [e.g., *Carey et al.*, 2010]. Askja was again active in the early 20th century, with at least

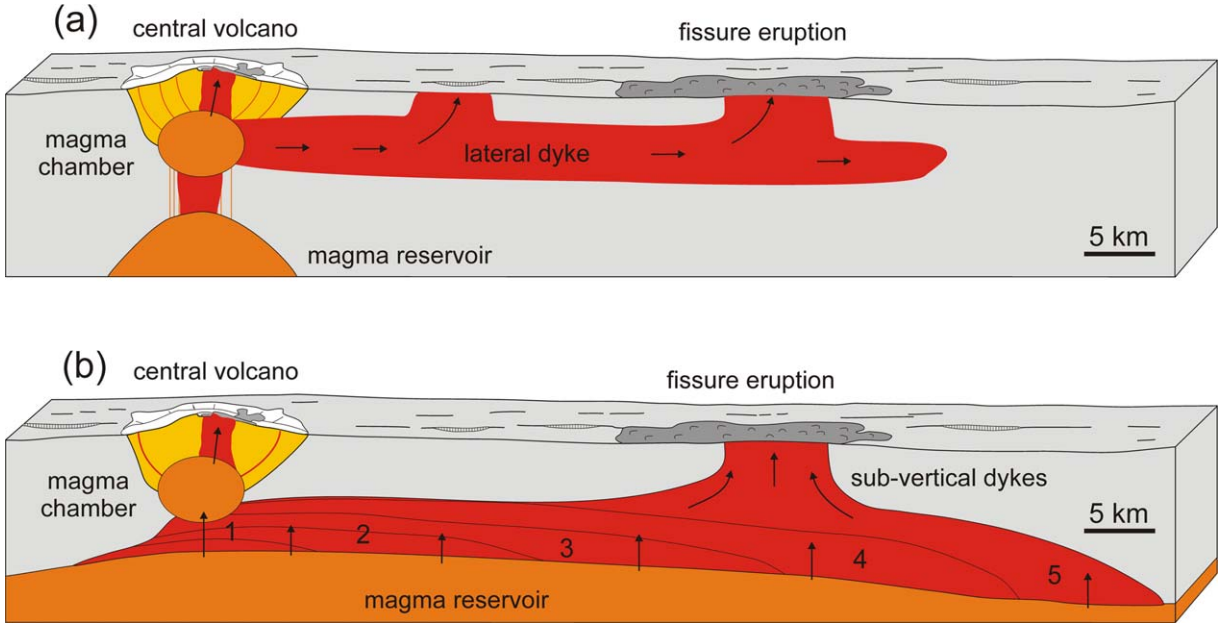

Figure 1. Schematic diagrams illustrating models of magma generation in Icelandic volcanic systems. (a) The lateral flow hypothesis considers that magma generation is focused beneath the central volcano. Fissure eruptions are fed by the injection of lateral dykes from shallow magma chambers beneath the central volcano. (b) The magma reservoir hypothesis considers that fissure eruptions on Icelandic volcanic systems are fed by subvertical dykes sourced from elongate magma reservoirs at the base of the crust. The numbers indicate the growth sequence of a vertical dyke from the magma reservoir. Upwelling magma does not necessarily interact with shallow crustal magma reservoirs prior to eruption. Modified after *Gudmundsson* [1987b].

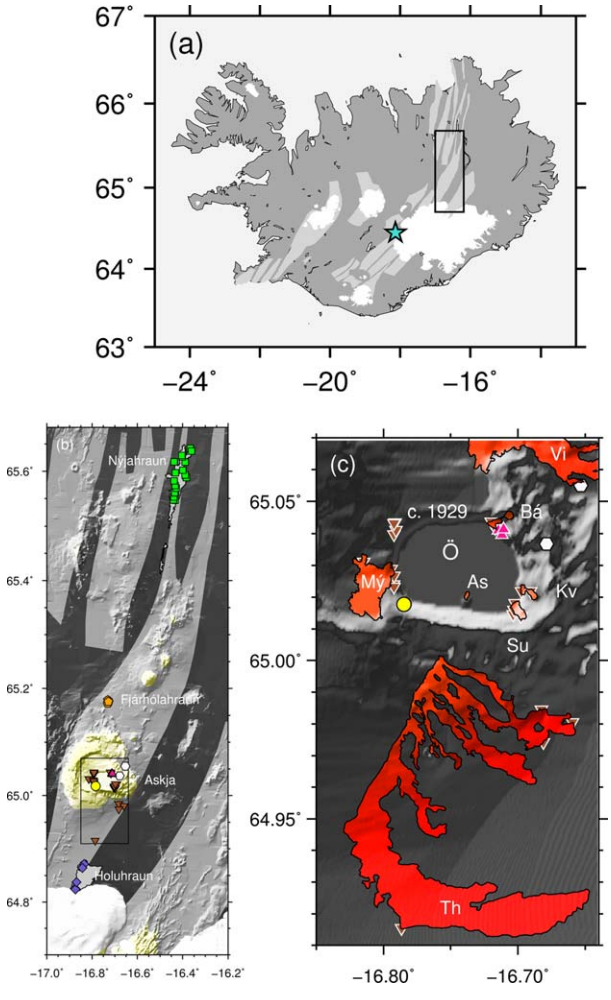

Figure 2. (a) Tectonic map of Iceland. The blue star shows the location of the Tröllahraun lava flow on the Veiðivötn volcanic system. (b) Tectonic map of the Askja volcanic system showing the locations of samples used in this study. Green squares, Nýjahraun; orange pentagons, Fjárhólahraun; pink triangles, NE tuff cone; yellow circles, SW tuff cone; white hexagons, basaltic tephra from January 1875; brown inverted trianges, Askja 20th century eruptions; blue diamonds, Holuhraun. (c) Map of the early 20th century eruptions along caldera ring flanks surrounding Öskjuvatn caldera (Ö): Bá, 1921 Bátshraun; Mý, 1922 Mývetningahraun; Kv, 1922/23 Kvíslahraun; Su, 1922/23 Suðurbotnahraun; As, 1926 Askur island. Thorvaldshraun (Th) erupted from a fissure on Askja's southern flanks that was intermittently active between 1924 and 1929. The 1961 Vikrahraun lava (Vi) is also shown.

six small-volume basaltic eruptions occurring along caldera ring fractures surrounding the Öskjuvatn caldera that formed following the 28–29 March 1875 eruption, and one fissure eruption on Askja's southern flank (Figure 2c).

[4] Previous workers have explained the similarity between the whole-rock major element compositions of the Nýjahraun lava and the Askja 20th century basalts in terms of the lateral flow hypothesis, suggesting that the eruptions at Sveinagjá were fed by the lateral flow of magma from Askja central volcano northward along the fissure swarm [*Sigurðsson and Sparks*, 1978a, 1978b; *Macdonald et al*., 1987]. The inferred lateral dyke was also used to explain the volume of caldera collapse at Öskjuvatn following the 28–29 March 1875 eruption, which far exceeds the volume of erupted products from this event. However, investigation of historical records detailing the growth history of Öskjuvatn caldera demonstrates that lateral flow is not required to explain its formation [*Hartley and Thordarson*, 2012], carrying the implication that the Nýjahraun eruptions were not necessarily directly linked to Askja by lateral magma supply. In this study, we re-examine the evidence for lateral flow during the 1874–1876 volcano-tectonic episode in light of new compositional data from whole-rock samples, matrix glasses, phenocrysts and melt inclusions from sample locations spanning the length of the Askja volcanic system.

2. Magmatic Plumbing in Icelandic Fissure Systems

2.1. Lateral Flow Hypothesis

[5] The lateral flow hypothesis was primarily developed to explain observations of laterally propagating seismicity in rift zones on volcanic edifices such as Hawaii [e.g., *Ryan*, 1988; *Parfitt and Wilson*, 1994] and at various mid-ocean ridges [e.g., *Dziak et al*., 1995; *Fialko and Rubin*, 1998; *Dziak et al*., 2004]. Most recently, seismic and magmatic activity in the Afar region of Ethiopia has been interpreted in terms of lateral magma injection [e.g., *Wright et al*., 2006; *Ebinger et al*., 2008; *Keir et al*., 2009; *Ayele et al*., 2009].

[6] Lateral flow was first applied to Icelandic volcanic systems by *Björnsson et al*. [1977] and *Einarsson and Brandsdóttir* [1979], in response to the Krafla Fires rifting episode of 1975–1984. Earthquake swarms beginning at Krafla and propagating northward for tens of km were interpreted as lateral magma intrusions from the Krafla magma reservoir into the fissure swarm [*Einarsson and Brandsdóttir*, 1979; *Buck et al*., 2006]. *Sigurðsson and Sparks* [1978a] later noted that fissure eruptions on volcanic systems close to the inferred centre of the Iceland plume (i.e., Katla, Grímsvötn and Askja) often produced large volumes of relatively evolved basalts with

compositions compatible with low-pressure fractional crystallization, and argued that these magmas must have been stored in shallow crustal reservoirs beneath central volcanoes. Fissure eruptions thus result from the extension of crustal fractures into shallow magma chambers, allowing fractionated magmas to flow laterally into the fissure swarm (Figure 1a) [*Sigurðsson and Sparks*, 1978a, 1978b].

[7] This model implies that magma upwelling is focused at the central volcano. During rifting episodes when compressive stresses are at a minimum, the overpressures generated by replenishment of shallow magma chambers may be sufficient to create fluid-driven cracks that propagate laterally along the fissure swarm. If the overpressure actively forces the outward injection of magma, then lateral magma flow may be viewed as a driving mechanism of the rifting observed out on the fissure swarm.

2.2. Magma Reservoir Hypothesis

[8] The magma reservoir hypothesis considers that, during rifting episodes, failure begins at a point of high tensile stress and propagates laterally along the strike of the volcanic system, enabling the buoyant rise of magma into new crustal fractures [*Gudmundsson*, 1995]. Fissure eruptions thus result from vertical to subvertical dykes rupturing the surface, and may occur close to, or many kilometres from, the central volcano [*Gudmundsson*, 1995]. These dykes ultimately tap large, elongate magma reservoirs underlying volcanic systems, with the top of the melt source region lying at the base of the crust [*Gudmundsson*, 1987a]. If tensile failure occurs beneath a central volcano, then upwelling magma is likely to intersect a shallow crustal magma chamber, which may trigger an eruption at the central volcano. While the dyke fracture propagates along strike, as evidenced by the laterally propagating seismicity, the magma flow itself is primarily vertical [*Gudmundsson*, 1995]. Lateral flow of magma from shallow crustal reservoirs into the fissure swarm is limited (Figure 1b).

3. Samples and Analytical Methods

[9] To ensure a thorough geochemical investigation of the products of the 1874–1876 volcano-tectonic episode, we conducted a detailed sampling campaign covering the length of the Askja volcanic system (Figure 2). On the Askja fissure swarm, we obtained samples from Nýjahraun and from two further fissure eruptions, Fjárhólahraun and Holuhraun, that are known to be young in age and have previously been interpreted as being associated with the 1874–1876 episode [e.g., *Carey et al*., 2010]. At Askja central volcano, samples were obtained from each of the small-volume basaltic eruptions of the early 20th century (Figure 2). We also consider samples from two phreatomagmatic tuff cone sequences, located on the north-eastern and south-western shores of Öskjuvatn, that represent some of the most primitive basalts found at Askja central volcano [*Hartley*, 2012]. Finally, we obtained basaltic fragments from the 1875 rhyolitic tephra, and sampled a thin basaltic tephra layer found immediately beneath the 1875 rhyolitic tephra that represents precursory activity from January 1875.

[10] Wherever possible, whole-rock compositional data were obtained for both lava and tephra samples. Whole-rock major and trace element data were obtained by X-ray fluorescence spectrometry. Analyses were performed using a Philips PW2404 automatic XRF spectrometer at the University of Edinburgh following the method of *Fitton et al*. [1998] with the modifications noted by *Fitton and Godard* [2004]. Whole-rock rare earth element (REE) concentrations were determined on a subset of samples by inductively coupled plasma mass spectrometry at the Scottish Universities Environmental Research Centre, East Kilbride. The samples were prepared using a HF/HNO_3-HNO_3-HCl tri-acid digestion procedure similar to that of *Olive et al*. [2001], and were analyzed using a VG Elemental PQ2 Plus quadrupole-based ICP-MS. The compositions of glassy tephra samples were determined by Cameca SX100 electron microprobe (WDS) at the University of Edinburgh using the method of *Hayward* [2012], and the same instrument was used to measure the compositions of olivine, clinopyroxene and plagioclase phenocrysts and microphenocrysts. We also analyzed naturally quenched olivine- and plagioclase-hosted melt inclusions from Holuhraun, Nýjahraun and the two Askja tuff cones. The melt inclusions ranged from 20 to 120 μm in size on their longest axis and consisted of homogenous glassy material. Some melt inclusions contained vapour bubbles. Major element compositions of the melt inclusions and their host crystals were measured by electron microprobe. Rare earth and selected trace element abundances in the melt inclusions and for selected matrix glasses were determined using the Cameca ims-4f ion microprobe at the University of Edin-

burgh. Full compositional data and details of all analytical methods are provided in supplementary information.

3.1. Eruption Ages

[11] All the eruptions considered in this study have previously been suggested to be associated with the 1874–1876 volcano-tectonic episode [*Carey et al*., 2010, and references therein], and this is the first study to test these suggestions in light of geochemical data. However, it is also important to determine the ages of these eruptions as accurately as possible. Many of the eruptions considered here can be dated very accurately using written historical accounts of volcanic activity in North Iceland: for example, most of the eruptions at Askja in the early 20th century can be dated to within a few months. A careful examination of historical records, and in some cases tephrochronological dating, reveals that some of these eruptions may be significantly older than 1875.

[12] The tuff cones on the NE and SW shores of Oskjuvatn are unconformably overlain by rhyolitic tephra from the 1875 eruption along much of their exposure. This has to previous suggestions that they may have been formed during precursory activity to the 28–29 March 1875 eruption [e.g., *Carey et al*., 2010]. However, at a single location the NE tuff sequence is overlain by two thin lava flows and a sediment pile containing several tephra layers, the oldest of which has been geochemically identified as the Hekla 3 tephra [*Hartley*, 2012], dated at 2.9 ka BP [*Larsen and Thorarinsson*, 1977]. Furthermore, the ~3.6 ka Sn2 and ~4.2 ka Hekla 4 tephra layers are absent from this profile. This places important age constraints on the underlying tuff deposits: they must have formed between 3.6 and ~3.0 ka BP. Such age constraints cannot be placed on the SW tuff sequence, other than that it is older than AD 1875 and that its appearance and preservation state are similar to the NE tuff cone.

[13] The age of the Holuhraun lava has been variously given as AD 1787 [*Sigurðsson and Sparks*, 1978b]; 1797 [*Siebert et al*., 2010]; 1875 [*Sigvaldason*, 1979], and as being connected with the 1874–1876 Askja volcano-tectonic episode [*Carey et al*., 2010]. Field observations and examination of aerial photographs and satellite images suggest that Holuhraun was formed in two separate eruptions. The older "Holuhraun-1" lava was erupted from a 2 km-long fissure located ~15 km south of Askja, while the younger "Holuhraun-2" lava erupted from a fissure that begins 23 km south of Askja and extends southward beneath Dyngjujökull glacier. Historical accounts can be used to tentatively date these lavas. It is known that new lava was erupted north of Dyngjujökull between 1794 and 1835, where previously only a sandy sediment cover had existed [*Jónsson*, 1945]. The eruption that produced this lava, Holuhraun-1, most probably occurred over the winter of 1797. Holuhraun-2 is possibly associated with fiery eruptions seen in the Dyngjujökull region between 1862 and 1864. If this is the case, then the Holuhraun-2 fissure was active at the same time as the Tröllagígar fissure on the Veiðivötn volcanic system. The Tröllagígar fissure was active between 1862 and 1864, and it produced the Tröllahraun lava. Tröllahraun is petrologically similar to Holuhraun, containing plagioclase macrocrysts and dispersed microphenocrysts of olivine, plagioclase and clinopyroxene set in a microcrystalline groundmass [*Thórarinsson and Sigvaldason*, 1972]. Because both Holuhraun-2 and Tröllahraun erupted from fissures very close to or extending beneath Vatnajökull, there is a possibility that a subglacial link exists between Holuhraun-2 and Tröllahraun: they may have erupted during a single volcano-tectonic event and may share a common magma source. Therefore we also examine the composition of Holuhraun in light of that obtained for Tröllahraun. This may allow further constraints to be placed on the age of Holuhraun-2, and determine whether Holuhraun-2 is connected to the 1874–1876 Askja volcano-tectonic episode. It should be noted that lavas and tephras from Holuhraun-1 and Holuhraun-2 are geochemically indistinguishable from one another, and so for much of the following discussion, Holuhraun is treated as a single entity.

[14] Fjárhólahraun erupted from a ~4 km-long fissure located ~25 km north of Askja. Rhyolitic tephra from the 28–29 March 1875 eruption lies immediately above fresh scoria from the Fjárhólar eruption. Historical accounts record that two eruption columns were visible from eastern Iceland in late December 1874 and early January 1875, one of which originated from an eruption site within Askja. Accounts written by observers in eastern Iceland state that the distance between the two columns was slightly greater than the distance between Askja and Herðubreið [*Gunnarsson*, 1875], i.e., ~20 km. Based on these descriptions, it was previously argued that one eruption column originated at Askja and that the second column was located south of Askja in the region of the Holuhraun cone rows, thereby linking Holuhraun-2

with the 1874–1876 volcano-tectonic episode [e.g., *Sigvaldason*, 1979]. However, written accounts from northern Iceland can only be reconciled with the eastern Iceland accounts if the second eruption column was located NNE of Askja, in the region between Askja and Herðubreið [*Brandsdóttir*, 1992]. It has therefore been postulated that the Fjárhólahraun lava is associated with the second eruption column north of Askja [e.g., *Carey et al*., 2010], and thus dates from early 1875.

[15] A thin layer of basaltic tephra occurs immediately below the 1875 tephra in various localities across the Öskjuop, preserved either as a thin band of fine ash or in discrete lenses. This tephra has a bimodal composition, and contains grains with Askja-like and Grímsvötn-like compositions [*Hartley*, 2012]. Through analysis of historical records it can be inferred with a degree of confidence that the Grímsvötn grains are from the relatively large eruption at Grímsvötn in January 1873, which dispersed tephra over the Askja region. The Askja grains must therefore be of a similar age, and are here taken to have originated from precursory activity on 1–3 January 1875.

4. Petrological Descriptions

[16] The main petrological and textural features of Holuhraun, Nýjahraun, Fjárhólahraun and the Askja 20th century basalts are summarized in Table 1 and Figure 3. While Fjárhólahraun and the Askja 20th century basalts are characterized by low-modal phenocryst abundances ($\leq$2 vol.%) and an almost-opaque, micro- to cryptocrystalline groundmass, Holuhraun and Nýjahraun are characterized by their high modal phenocryst abundances ($<$15 vol.%).

[17] Holuhraun lava samples are characterized by the abundance of plagioclase phenocrysts and the occurrence of large glomerocrysts ($\sim$4 to 8 mm in diameter). Some glomerocrysts are comprised almost entirely of plagioclase (Figure 3a), while others contain aggregates of plagioclase, acicular black clinopyroxene and minor olivine (Figure 3b). The glomerocrysts are most abundant in the northern section of the Holuhraun cone row, and are particularly apparent in scoria and spatter bombs found close to the cone row. By contrast, in typical lava samples from Nýjahraun, phenocrysts, and microphenocrysts of plagioclase, clinopyroxene, and olivine occur in isolation (Figure 3c). Glomerocrysts are present in Nýjahraun lavas (e.g., Figure 3d), but the crystals in these aggregates tend to be smaller than individual phenocrysts.

[18] The Holuhraun phenocryst and glomerocryst assemblage is similar to that commonly found in lavas of the Bárðarbunga-Veiðivötn volcanic system [*Jakobsson*, 1979; *Hansen and Grönvold*, 2000; *Halldorsson et al*., 2008]. The plagioclase macrocrysts ($>$0.7 mm) in these lavas are suggested to have originated in mid- to deep-crustal gabbroic mush bodies formed during intrusive events, and were subsequently entrained in ascending magmas during crustal rifting episodes [*Hansen and Grönvold*, 2000; *Halldorsson et al*., 2008].

5. Geochemical Variability in Askja Samples

5.1. Whole-Rock

[19] The lava and tephra formations of this study fall into two broad compositional groups (Figure 4). The more primitive samples contain 49.8–50.5 wt.% SiO_2, 7.0–7.3 wt.% MgO, and 1.64–1.72 wt.% TiO_2; this group includes the Askja NE tuff cone, Holuhraun and Tröllahraun. Samples from the SW tuff cone are slightly more evolved, but may still be considered to fall within the "primitive" cluster. Samples from Nýjahraun, Fjárhólahraun and the Askja 20th century basalts are more evolved, and contain 50.0–51.6 wt.% SiO_2, 4.6–5.4 wt.% MgO, and 2.60–2.85 wt.% TiO_2. Tephra from the January 1875 precursor eruptions is compositionally different from Nýjahraun and the Askja 20th century basalts, and falls outside the "evolved" compositional group.

[20] Eruptions within the "primitive" compositional group may be distinguished from one another using major element ratios. In particular, whole-rock samples from Holuhraun and Tröllahraun have higher TiO_2/K_2O than the two Askja tuff cones (Figure 4b). TiO_2/K_2O is expected to remain approximately constant while olivine and plagioclase are liquidus phases, and to decrease slowly as clinopyroxene joins the crystallizing assemblage. However, once titanomagnetite or ilmenite become liquidus phases, TiO_2/K_2O will decrease rapidly as Ti is partitioned into oxide minerals. TiO_2/K_2O is therefore indicative of variations in the modal proportions of oxide minerals in different magmas. High TiO_2/K_2O in Holuhraun and Tröllahraun indicates that oxide crystallization

Table 1. Textural and Petrological Descriptions of Askja Lavas and Tephras[a]

Eruption	Texture	Phase	Phenocrysts	Microphenocrysts	Groundmass	Tephra
Holuhraun	Holuhraun typically has a holocrystalline, subophitic to intergranular texture containing dispersed microphenocrysts of plagioclase, olivine and clinopyroxene. It contains large glomerocrysts ranging from 4 to 8 mm in diameter.		≤15 vol.%		Microcrystalline	Glassy
		plg	Abundant; 1–5 mm	≤1 mm	x	Feathery microlites
		olv	Common; 0.5–2 mm	≤0.4 mm		
		cpx	Rare; 0.5–2 mm	≤0.6 mm	x	Feathery microlites
		Fe-Ti oxides			x	
Nýjahraun	Nýjahraun typically has a holocrystalline, porphyritic texture. The almost-opaque groundmass appears tachylitic under plane-polarsied light but is revealed to be microcrystalline when viewed under reflected light. Glomerocrysts are normally smaller than individual phenocrysts.		≤13 vol.%[b]		Cryptocrystalline	Glassy
		plg	Abundant (6.7%); 1.5–2 mm	≤1.0 mm	x	Rare microlites
		olv	Rare (0.5%); 0.5–2 mm			
		cpx	Common (4.8%); ∼1.5 mm	≤0.8 mm	x	Rare microlites
		Fe-Ti oxides		∼0.3 mm	<6 μm	
Fjárhólahraun	Fjárhólahraun is typically holocrystalline and displays a trachytic groundmass texture. It contains rare tabular plagioclase phenocrysts, and abundant microphenocrysts that form small (<500 μm) glomerocrysts.		∼2 vol.%		Microcrystalline	Glassy
		plg	Rare; ≤2 mm	≤0.8 mm	Acicular	Rare microlites
		olv				
		cpx		≤0.8 mm	x	Rare microlites
		Fe-Ti oxides			x	
Askja 20th century	The Askja 20th century lavas are holocrystalline and have uniformly low modal phenocryst abundances. Rare tabular plagioclase phenocrysts are found in Bátshraun and Kvíslahraun samples. All the Askja 20th century lavas have an almost-opaque, micro- to cryptocrystalline groundmass.		<1 vol.%		Cryptocrystalline	Glassy
		plg	Rare; ≤2 mm	≤0.8 mm	≤10 μm	Rare microlites
		olv				
		cpx		≤0.8 mm	≤10 μm	Rare microlites
		Fe-Ti oxides			≤10 μm	

[a]Phases: plg, plagioclase; olv, olivine; cpx, clinopyroxene.
[b]Nýjahraun modal phenocryst abundances from *Sigurðsson and Sparks* [1978b].

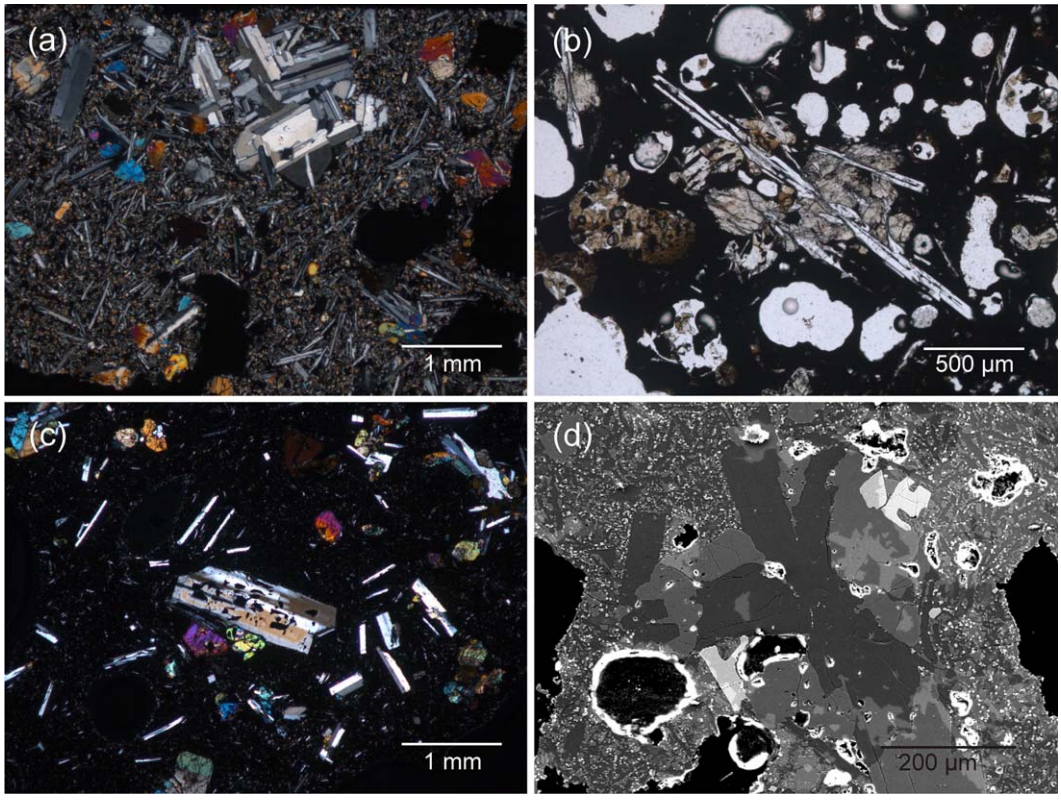

Figure 3. Representative photomicrographs of samples used in this study. (a) Holuhraun; cross-polarized light. Plagioclase glomerocryst in holocrystalline groundmass. (b) Holuhraun; plane-polarized light. Glomerocryst of elongate laths of plagioclase surrounded by smaller, sub-equant olivine and clinopyroxene. (c) Nýjahraun; cross-polarized light. A large, isolated plagioclase phenocryst surrounded by microphenocrysts of olivine, plagioclase and clinopyroxene. The groundmass is almost opaque and appears to be hypohyaline. (d) Nýjahraun; SEM image. Glomerocryst of plagioclase and clinopyroxene surrounded by holocrystalline groundmass. Note the abundance of bright white Fe-Ti oxides, present as microphenocrysts and in the groundmass.

from these magmas was not significant, while the low TiO_2/K_2O of Nýjahraun, Fjárhólahraun and the Askja 20th basalts is indicative of significant crystallization of oxides as liquidus phases in these magmas. This is consistent with petrographic observations: Holuhraun samples contain very few oxide minerals, while iron-titanium oxides are abundant in Nýjahraun and the Askja 20th century basalts.

[21] Trace element ratios also distinguish between different eruptions in the "primitive" and "evolved" compositional groups. Ratios of compatible trace elements such as Cr and Ni are particularly useful in distinguishing different eruptions within the primitive cluster (Figure 4c). Holuhraun has the highest Ni abundance (61.9±4.4 ppm) and lowest Cr/Ni ratio (1.08±0.08) of the primitive cluster, while the two tuff cones have lower Ni abundances (55.1±2.5 ppm for the NE tuff cone) and higher Cr/Ni ratios (2.25±0.11 for the SW tuff cone).

[22] Within the "evolved" compositional cluster, Nýjahraun whole-rocks are slightly enriched in Cr and Ni in comparison to the Askja 20th century basalts: Nýjahraun samples contain 33.2±3.2 ppm (1σ) Ni, while the Askja 20th century basalts contain 25.4±3.3 ppm Ni. This may be explained by the abundance of Ni-bearing olivine and Cr-bearing clinopyroxene in the Nýjahraun samples. By contrast, the Askja 20th century basalts are essentially aphyric, and so have lower abundances of those elements that are compatible in phenocryst phases during crystallization. Nýjahraun also has lower ratios of incompatible to compatible elements, such as Zr/Ni, than the Askja 20th century basalts and Fjárhólahraun (Figure 4d). However, these ratios are not able to distinguish Fjárhólahraun samples from the Askja 20th century basalts.

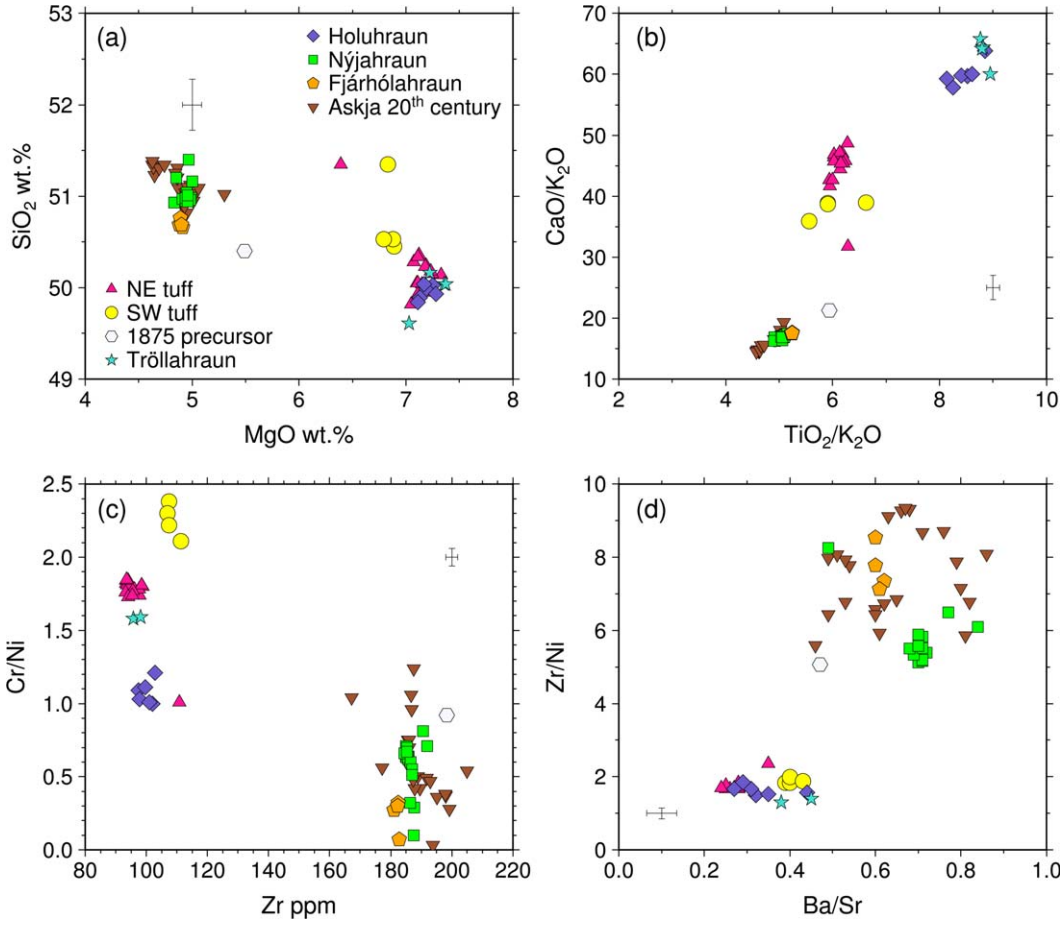

Figure 4. Whole-rock compositional variations in samples from the Askja volcanic system, determined by XRF analysis. There are two discrete clusters of "primitive" and "evolved" samples. Individual eruptions within the evolved cluster cannot be distinguished from one another on the basis of their major or trace element concentrations and ratios. In the primitive cluster, the Askja tuff cones can be distinguished from Holuhraun and Tröllahraun using certain major and trace element ratios. Error bars show 1σ precision estimates based on repeat analyses of standards.

[23] The Askja 20th century basalts have a much wider range in incompatible trace element ratios, such as Ba/Sr, than Nýjahraun (Figure 4d). It is interesting to note that the Askja 20th lavas with the highest Ba/Sr values are situated near active geothermal sites on or around the shores of Öskjuvatn lake. Elements such as Sr, Rb, and K are fluid-mobile during low-grade zeolite-facies metamorphism [e.g., *Wood et al*., 1976]; therefore, it is possible that the Askja 20th century lavas with higher Sr, Rb, K_2O, and Ba/Sr have been slightly modified by hydrothermal alteration, despite the fresh appearance of the samples collected.

5.2. Glass

[24] Analyses of glassy tephras reveal compositional differences between eruptions that are not apparent in the whole-rock data. Nýjahraun glasses are the most evolved of all the samples considered, and are easily distinguished from the "pre-1875" tephra and the Askja 20th century eruptions in oxide-oxide plots (Figure 5). In some cases, glass from a single eruption shows a much greater compositional variability than whole-rock analyses from that eruption. This is most evident in glasses from the SW tuff cone and the "pre-1875" basaltic tephra (Figure 5). The variability in glass compositions means that the "primitive" and "evolved" compositional clusters observed in the whole-rock data are not retained in the glass data. The pre-1875 tephras in particular have compositions that are intermediate between the more primitive and the more evolved eruptions.

[25] Major element ratios enable some eruptions to be distinguished from one another. Both P and K behave as incompatible elements in a

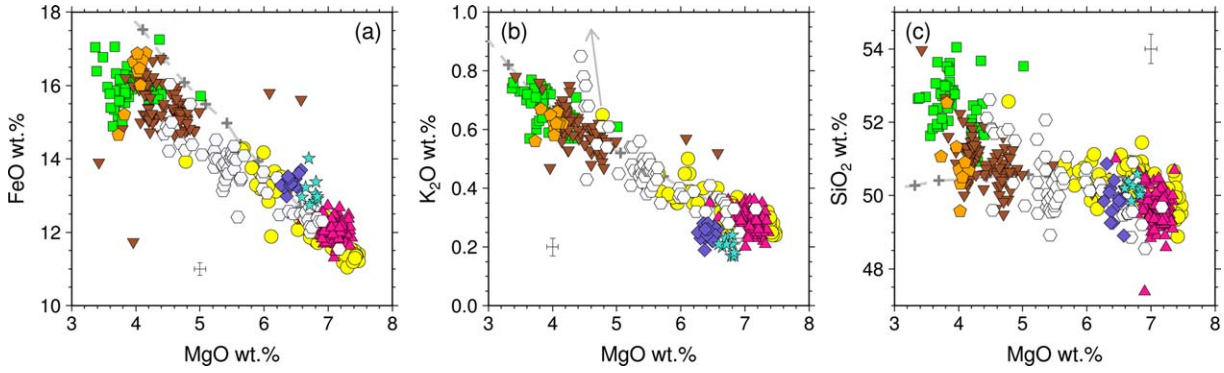

Figure 5. Oxide-oxide plots showing major element variations in glassy tephras from the Askja volcanic system, using same symbols as Figure 4. Liquid lines of descent (gray dashed lines) were calculated with Comagmat [*Ariskin et al*., 1993] using the average (mean) glass composition of the NE tuff cone as a starting composition. Increments of 5% crystallization are marked by crosses. The gray arrow in (b) indicates a mixing trend between the "pre-1875" tephra (white symbols) and composition of Askja rhyolite. Error bars show 1σ precision estimates based on repeat analyses of standards.

crystallizing basaltic magma, and are both incompatible in ilmenite and titanomagnetite; thus, P_2O_5/K_2O is expected to remain approximately constant during fractional crystallization, or to increase slightly if K is partitioned into plagioclase. This means that P_2O_5/K_2O can be a useful indicator of the source magma composition. The Nýjahraun glasses can be distinguished from the Askja 20th century basalts by their higher CaO/K_2O for a given P_2O_5/K_2O (Figure 6a) and for a given K_2O content (Figure 6c).

[26] Glasses from Holuhraun and Tröllahraun are characterized by $TiO_2/K_2O>7$, while samples from other eruptions generally have lower TiO_2/K_2O (Figure 6b). Similarly, Nýjahraun, Fjárhólahraun and Askja 20th century basalts are characterized by $CaO/K_2O<20$. Least-squares regression lines calculated for plots of CaO/K_2O versus TiO_2/K_2O suggest that Nýjahraun and the Askja 20th century basalts plot on different gradients, indicative of differing degrees of crystallization of titanium-rich oxides. However, for TiO_2/K_2O ratios of ~0.5, these differences are not resolvable within the 1σ uncertainty of the analyses.

[27] The ratio TiO_2/FeO can be used to distinguish between basalts from different volcanic systems in Iceland [*Óladóttir et al*., 2008; *Jagan*, 2010, and references therein]. For a given K_2O content, basalts originating from the Bárðarbunga-Veiðivötn and Grímsvötn volcanic systems have higher TiO_2/FeO than basalts from the Askja volcanic system [e.g., *Jagan*, 2010]. At K_2O contents of ~0.25 wt.%, glasses from Holuhraun and Tröllahraun have higher TiO_2/FeO than glasses from the Askja tuff cones (Figure 6d).

[28] In all the major element ratios shown in Figure 6, the pre-1875 tephra bridges the compositional gap between the older, "primitive" glasses of the Askja tuff cones and the younger, "evolved" glasses from Nýjahraun and the Askja 20th century eruptions. In this light, it is interesting to note that while the 1875 precursors and Nýjahraun and are time-equivalent magmas (pre-1875 eruptions occurred in January 1875; Nýjahraun eruptions began in February 1875), yet have very different compositions.

5.3. Mineral Chemistry

[29] The relationship between phenocrysts and their carrier melts can be investigated by comparing the observed cation partitioning between a crystal phase and its host melt with the behaviour expected under chemical equilibrium. Experimental data indicate that, for basaltic melts, equilibrium olivine-liquid pairs have expected Kd^{ol-liq}_{Fe-Mg} values between 0.27 and 0.35 [*Roeder and Emslie*, 1970; *Ford et al*., 1983; *Grove et al*., 1992; *Putirka*, 2005]. Expected equilibrium clinopyroxene-liquid $Kd^{cpx-liq}_{Fe-Mg}$ values are 0.27 ± 0.03 [*Putirka*, 1999], and equilibrium plagioclase-liquid pairs are expected to have $Kd^{plg-liq}_{Na-Ca}$ between 1.0 and 1.3 [*Grove et al*., 1992]. Plots of mineral-melt pairs are provided in supplementary information, Figure S1.

[30] All the samples considered in this study contained tabular plagioclase phenocrysts with highly

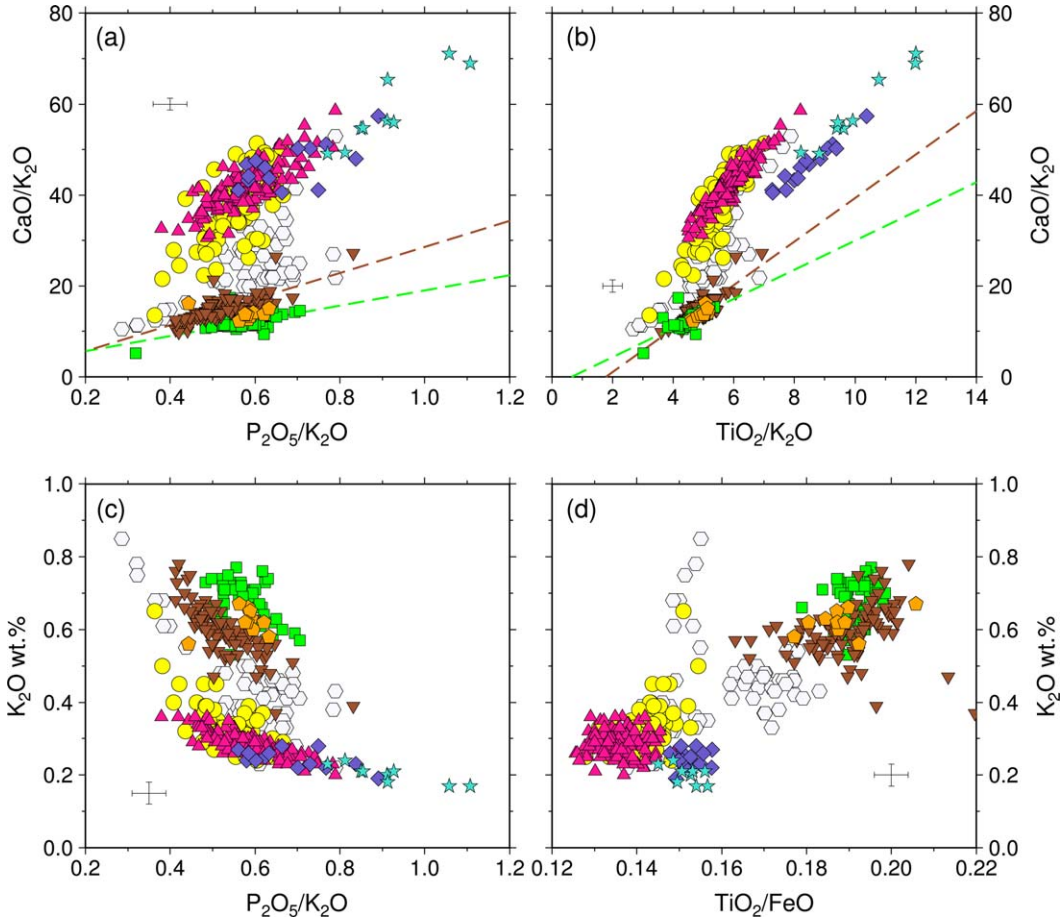

Figure 6. Major element ratios in glasses from the Askja volcanic system, using same symbols as Figure 4. (a) and (c) Glasses from Nýjahraun can be distinguished from those of the Askja 20th century eruptions on the basis of P_2O_5/K_2O. (b) Holuhraun and Tröllahraun are distinguished by $TiO_2/K_2O>7$, while the evolved Askja, Nýjahraun and Fjárhólahraun samples have $CaO/K_2O<20$. The Askja 20th century basalts and Nýjahraun appear to fall on different trends indicated by coloured dashed lines, but these may not be used as distinguishing compositional features given the analytical uncertainty of the measurements. (d) Holuhraun and Tröllahraun have higher TiO_2/FeO than the Askja tuff cones for a given K_2O content. Error bars show 1σ precision estimates based on repeat analyses of standards.

anorthitic crystal cores (~An_{80}-An_{90}), with the exception of Fjárhólahraun (Figure 7a). Only Holuhraun and Nýjahraun contained large olivine phenocrysts, with compositions up to Fo_{86} (Figure 7b). The clinopyroxenes analyzed in this study have a limited compositional range, but define two distinct populations (Figure 7c). Clinopyroxenes from Nýjahraun, Fjárhólahraun and the Askja 20th century basalts are compositionally very similar, while clinopyroxenes from Holuhraun are more Fe-rich.

[31] Plagioclase crystals from Holuhraun fall into two distinct clusters of An_{88}-An_{76} and An_{70}-An_{59} (Figure 7a). The more anorthitic plagioclases often exhibit normal or oscillatory zoning. Core compositions are typically in the range An_{86}-An_{81}, and many crystals have thin, albitic rims with compositions between An_{68} and An_{60} that are in equilibrium with the Holuhraun glass composition ($Kd^{plg-liq}_{Na-Ca}$ between 1.0 and 1.35). Olivines from Holuhraun range between Fo_{86} and Fo_{70} (Figure 7b). The mean olivine composition is Fo_{80}, and approximately 25% of the olivines analyzed have compositions in the range Fo_{82} to Fo_{86}. Assuming a Kd^{ol-liq}_{Fe-Mg} of 0.3, the average Holuhraun glass composition is in equilibrium with Fo_{75} olivine; thus, the majority of olivines analyzed were not in equilibrium with the carrier melt at the time of eruption. The more forsteritic olivines in the Holuhraun lava therefore crystallized from a more primitive melt composition, and were mobilized

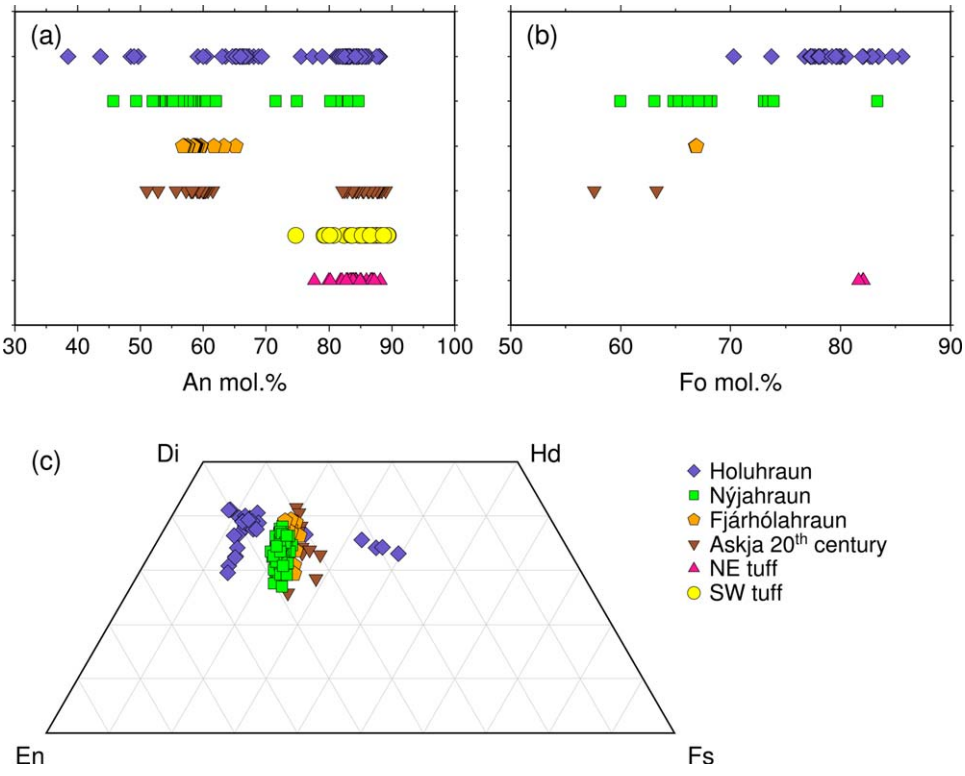

Figure 7. Compositions of (a) plagioclase, (b) olivine, and (c) clinopyroxene phenocrysts, microphenocrysts and groundmass crystals for samples from the Askja volcanic system. The symbols are larger than the 1σ error bars.

with the magma during eruption. Clinopyroxene is found as an isolated phenocryst phase in Holuhraun lava samples, but is rare. Black, augitic clinopyroxenes present within glomerocrysts span a narrow compositional range from $En_{46}Fs_{13}Wo_{41}$ to $En_{56}Fs_{14}Wo_{31}$ (Figure 7c), and have no significant compositional zoning.

[32] Plagioclases from both NE and SW tuff sequences have highly anorthitic crystal cores ranging in composition from An_{85} to An_{89} (Figure 7a). Almost all of the plagioclases analyzed exhibit oscillatory zoning, with crystal rims slightly more sodic than the crystal cores. Plagioclase rim compositions ranged from An_{88} to An_{75}. None of the phenocrysts analyzed had rims with compositions in equilibrium with the tuff cone glass compositions.

[33] The majority of plagioclases from Nýjahraun have compositions between An_{62} and An_{52} (Figure 7a). Two microphenocrysts had more sodic compositions of An_{46} and An_{49}. Just over 11% of the plagioclases analyzed had anorthitic cores (An_{84}-An_{71}) and displayed normal or oscillatory zoning with thin, labradoritic (An_{57}-An_{53}) rims. The An_{62}-An_{52} phenocrysts have $Kd^{plg-liq}_{Na-Ca}$ between 0.98 and 1.35, and may thus be considered to be in equilibrium with their carrier melt. Nýjahraun olivines typically range between Fo_{74} and Fo_{60}, but there are a small number of larger, more forsteritic (up to Fo_{84}) olivines (Figure 7b). The olivine crystals with compositions between Fo_{63} and Fo_{68} have Kd^{ol-liq}_{Fe-Mg} between 0.29 and 0.34; thus, the main population of olivines can be considered to be in equilibrium with the Nýjahraun carrier melt. Clinopyroxenes from Nýjahraun have compositions between $En_{50}Fs_{22}Wo_{28}$ and $En_{43}Fs_{19}Wo_{38}$ (Figure 7c).

[34] The Askja 20th century basalts and Fjárhólahraun are essentially aphyric; thus, our dataset is dominated by microphenocryst and groundmass crystal compositions. Plagioclase microphenocrysts from Fjárhólahraun have compositions between An_{57} and An_{65}, and those from the Askja 20th century basalts range between An_{51} and An_{62} (Figure 7a). The Askja 20th century basalts may contain rare plagioclase phenocrysts with highly anorthitic crystal cores (An_{82}–An_{89}). Whilst these are compositionally similar to the high-anorthite plagioclases found in Nýjahraun and the two Askja

tuff cones, the anorthitic phenocrysts are much less abundant in the Askja 20th century basalts than in Nýjahraun. Rare olivine microphenocrysts (Fo_{57}–Fo_{67}) are present in Fjárhólahraun and the Askja 20th century basalts. Clinopyroxene microphenocrysts had compositions ranging from $En_{49}Fs_{25}Wo_{26}$ to $En_{39}Fs_{19}Wo_{42}$ (Figure 7c).

6. Fractional Crystallization Modelling

[35] The two Askja tuff cones are among the most primitive basalts yet analyzed from the Askja caldera [*Hartley*, 2012]. If the composition of glass from the NE tuff cone is taken to be broadly representative of primitive melts being supplied to Askja central volcano, then it is possible to investigate whether evolved basalts erupted at Askja can be generated by fractional crystallization of this primitive composition. To test this hypothesis, mass balance calculations were performed using the Comagmat crystallization model [*Ariskin et al*., 1993], taking the average glass composition of the NE tuff cone as a parental liquid composition. Calculations were performed assuming anhydrous conditions with oxygen fugacity set at 1 log unit below the quartz-fayalite-magnetite buffer, consistent with a Fe^{2+}/Fe^{T} ratio of 0.9 [*Óskarsson et al*., 1994] and with previous studies modelling the crystallization of basalts from North Iceland [e.g., *Maclennan et al*., 2002]. We tested crystallization pressures between 0.8 and 1.2 kbar, appropriate for crystallization in a shallow (~3 km depth) magma reservoir. The chosen pressure did not significantly affect the calculated liquid line of descent (LLD) or the modal mineralogy of the crystallizing assemblage.

[36] Approximately 40% crystallization of the starting melt composition was required to produce a liquid that matched the MgO content of the Askja 20th century glass compositions (Figure 5). After 40% crystallization the crystallizing assemblage contained plagioclase, clinopyroxene and olivine in the proportions 57:41:2. The calculated compositions of phenocrysts in equilibrium with the model residual liquid were Fo_{68} olivine, An_{59} plagioclase and $En_{43}Fs_{19}Wo_{27}$ clinopyroxene. These compositions closely match the microphenocryst compositions analyzed in the Askja 20th century basalt samples. The Comagmat model did not reproduce the crystallization of oxide minerals, which are liquidus phases in the Askja 20th century basalts according to petrographic observations. Consequently, the calculated liquid composition predicts higher FeO than is observed in the samples (Figure 5a).

[37] The fractional crystallization models did not reproduce the SiO_2 enrichment observed in Nýjahraun glasses compared to the pre-1875 and Askja 20th century glasses for a given TiO_2 or MgO content (Figure 5c). Silica enrichment only occurs in highly evolved Iceland basalts when titanomagnetite or ilmenite become liquidus phases [*Sigurðsson and Sparks*, 1981]. We therefore suggest that oxide minerals arrived on the liquidus of the Nýjahraun basaltic liquid earlier than for the Askja 20th century basalts, thus producing the observed SiO_2 enrichment enrichment for Nýjahraun. This implies that these two magmatic liquids did not derive from a common parental magma.

[38] The "pre-1875" basaltic tephra provides the best estimate of the composition of basaltic magma upwelling beneath Askja during the 1874–1876 volcano-tectonic episode. These tephras mostly fall on the calculated fractional crystallization trends (Figure 5); however, their compositional variability is wider than would be expected for fractional crystallization alone. The trend of K_2O enrichment evident in Figure 5b is best explained by the mixing of the pre-1875 basaltic magma with a small amount of an evolved contaminant enriched in K_2O, such as the rhyolitic magma resident beneath Askja at this time. The compositional variability in the pre-1875 tephra indicates that this mixing was imperfect and had not produced a homogeneous magma before the precursory eruptions in early January 1875.

[39] The Fjárhólahraun glasses are compositionally more similar to the Askja 20th century basalts than to Nýjahraun: they do not show the SiO_2 enrichment of Nýjahraun, and their compositions are reproduced by the calculated LLDs using the NE tuff cone glasses as a parental melt (Figure 5). These similarities leave open the possibility that Fjárhólahraun and the Askja 20th century basalts may have originated from a common parental magma.

7. Clinopyroxene-Liquid Thermobarometry

[40] The *Putirka* [2008] clinopyroxene-liquid thermobarometer was used to investigate clinopyroxene crystallization pressures and temperatures for the magmas erupted at Holuhraun, Nýjahraun, Fjárhólahraun, and two of the Askja 20th century eruptions: Kvíslahraun (1922–1923) and Thorvaldshraun (1924–1929). The 1σ calibration errors are $\pm 30°C$ and ± 1.5 kbar for the thermometer and

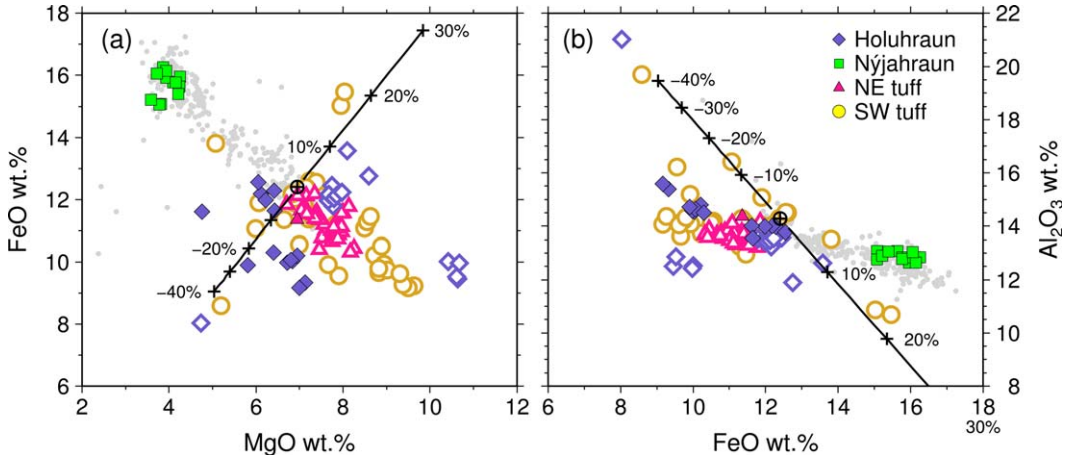

Figure 8. Oxide-oxide plots showing the compositional variability of olivine- and plagioclase-hosted melt inclusions from Holuhraun, Nýjahraun and the two Askja tuff cones. Olivine-hosted melt inclusions shown by coloured symbols; plagioclase-hosted melt inclusions shown by open symbols. The symbols are larger than the 1σ error bars. Glass compositions for these eruptions are shown in gray. None of the melt inclusions have been corrected for post-entrapment crystallization. The black lines are plagioclase control lines showing the effect of post-entrapment crystallization on a plagioclase-hosted melt inclusion from the SW tuff cone. Positive numbers show the amount of post-entrapment crystallization that could account for the composition of the melt inclusion, assuming that it crystallized An_{81} plagioclase containing 0.6 wt.% FeO, 0.22 wt.% MgO and 31.7 wt.% Al_2O_3. Negative numbers show the effect of plagioclase addition to the inclusion, i.e., post-entrapment melting.

barometer, respectively. For each eruption, the average tephra glass composition was considered to be representative of the magmatic liquid immediately prior to eruption. Clinopyroxene-liquid pairs were then filtered to remove pairs outwith the range $Kd^{cpx-liq}_{Fe-Mg} = 0.27 \pm 0.04$.

[41] Estimated crystallization temperatures for clinopyroxenes from Holuhraun were between 1128 and 1200°C, and crystallization pressures ranged from 2.3 to 7.6 kbar (see supplementary information, Figure S2). These pressures indicate that crystallization occurred primarily in the mid- to lower crust. The Nýjahraun clinopyroxenes crystallized at temperatures between 1116 and 1155°C, and pressures between 0.6 and 4.2 kbar (mean 2.85 kbar; see Figure S2). These pressures are somewhat lower than, but within the range of, previous estimates of Nýjahraun clinopyroxene crystallization depths of 12–18 km [*Sigvaldason et al*., 2002].

[42] Crystallization pressure estimates for clinopyroxene microphenocrysts from Fjárhólahraun were between 0.2 and 4.6 kbar (mean 2.84 kbar). Pressure estimates for the Kvíslahraun and Thorvaldshraun clinopyroxenes were between 0.3 and 5.2 kbar (mean 2.73 kbar). A population of clinopyroxene microphenocrysts from the Askja 20th century eruptions have very similar crystallization pressures to Fjárhólahraun and Nýjahraun. However, 25% of the Askja 20th century basalts also record much shallower crystallization pressures of <1.5 kbar (i.e., within the upper 5 km of the crust), compared to 14% and 16% of the Fjárhólahraun and Nýjahraun clinopyroxenes respectively. The distribution of clinopyroxene crystallization pressures suggests that it is possible to differentiate between Nýjahraun and the the Askja 20th century eruptions on the basis of clinopyroxene-liquid thermobarometry.

8. Melt Inclusions

[43] Major and trace element compositions of olivine-, plagioclase- and clinopyroxene-hosted melt inclusions from Holuhraun, Nýjahraun and the two Askja tuff cones were used to investigate the compositions of the source magmas of these eruptions. Hand-picked, inclusion-bearing phenocrysts from tephra samples were selected, and only naturally quenched, glassy melt inclusions were analyzed. Major element data for a subset of the melt inclusions included in this study are given in *Hartley et al*. [2012].

[44] The melt inclusions range from very primitive (>10 wt.% MgO) to very evolved (~4.0 wt.% MgO). All the melt inclusions from Nýjahraun were very evolved and had similar compositions to Nýjahraun glasses. Melt inclusions from Holuhraun and the two tuff cones show much greater

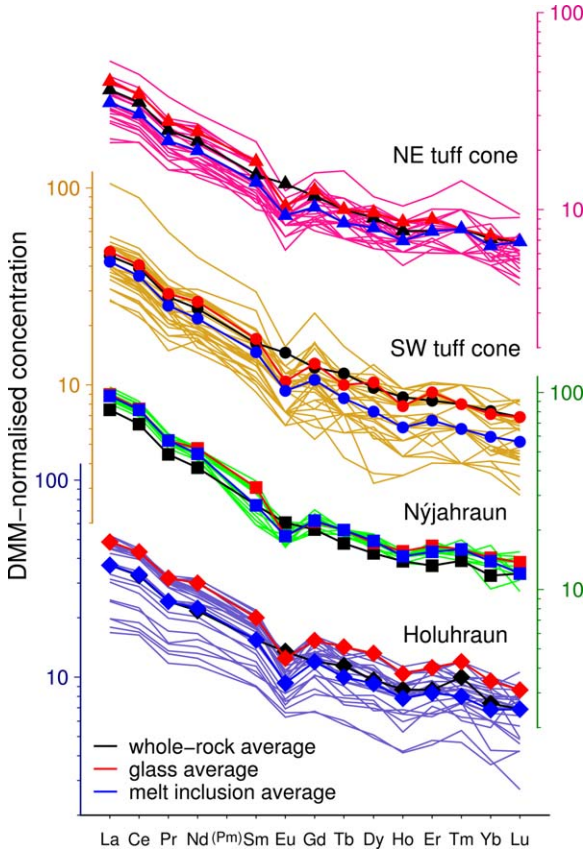

Figure 9. Rare earth element (REE) data for melt inclusions and their host eruptions. Concentrations are normalized to the depleted MORB mantle composition of *Workman and Hart* [2005]. Melt inclusion and glass data were obtained by SIMS, and preserve a negative Eu anomaly indicative of plagioclase crystallization. Whole-rock data were obtained by ICP-MS, and the expected Eu anomaly is removed by the data reduction procedure.

compositional variability than their carrier melts (Figure 8).

[45] We used Petrolog3 [*Danyushevsky and Plechov*, 2011] to determine the degree of post-entrapment crystallization (PEC) experienced by the olivine-hosted melt inclusions, and to restore the melt inclusions to their initial trapped compositions asuming a Kd^{ol-liq}_{Fe-Mg} of 0.3. Holuhraun melt inclusions experienced between 0.9 and 5.7% PEC (average 2.2%); Nýjahraun inclusions experienced between 1.9 and 4.7% PEC (average 3.3%). Post-entrapment effects in plagioclase-hosted melt inclusions were estimated by adding plagioclase of the same composition as the host crystal into the measured melt inclusion composition. Most plagioclase-hosted melt inclusions show minimal post-entrapment effects (<5% PEC); however, two melt inclusions from the SW tuff cone have undergone up to 20% PEC (Figure 8). Two plagioclase-hosted inclusions also appear to be affected by up to 40% plagioclase addition, i.e., the remelting of plagioclase into the melt inclusion as the crystal is entrained in a hotter carrier liquid (Figure 8). Fortunately, it is possible to use incompatible trace elements in melt inclusions without correction in order to investigate source melt compositions, since incompatible trace element concentrations in the melt inclusion will increase relative to the initial trapped composition as PEC progresses, but the ratios between them will be unaffected [e.g., *Starkey et al*., 2012].

[46] *Maclennan* [2008] has shown that diverse melt compositions generated in the Icelandic lower crust undergo concurrent mixing and crystallization in the crust during magma ascent, progressively homogenizing the melt compositions. Melt inclusions trapped in the most forsteritic olivines and the most anorthitic plagioclases are therefore expected to show the greatest compositional diversity, while inclusions in more evolved host crystals are more homogeneous in composition. The mean melt inclusion composition is also expected to be similar or identical to the composition of the carrier melt at the time of eruption. The most primitive olivine crystals analyzed in this study are too evolved to represent the very first stages of crystallization from a mantle melt; therefore these melt inclusions are unlikely to represent the true compositional diversity of melts supplied to the lower crust beneath Askja.

[47] For all the eruptions except the SW tuff cone, REE profiles for melt inclusions and glasses have similar slopes and La/Yb ratios (Figure 9), and the average melt inclusion La/Yb is very similar to the average of the carrier melt (Figure 10). This indicates that the melt inclusions from Holuhraun, Nýjahraun, and the NE tuff cone are consistent with a genetic relationship with their carrier melts. Melt inclusions hosted in the most primitive plagioclase crystals from Holuhraun and the NE tuff cone may preserve information about the composition of mantle melts supplied to these systems, but the small dataset prevents a detailed investigation of the compositional diversity of these melts. No primitive phenocrysts or melt inclusions from Nýjahraun were found in this study: the melt inclusions analyzed have identical major and trace element compositions to the Nýjahraun glass (Figure 8). This is consistent with these melt inclusions being trapped during late-stage crystallization in the mid- to upper crust; thus, they do not preserve information about the compositions of mantle melts supplied to Nýjahraun. Melt inclusions

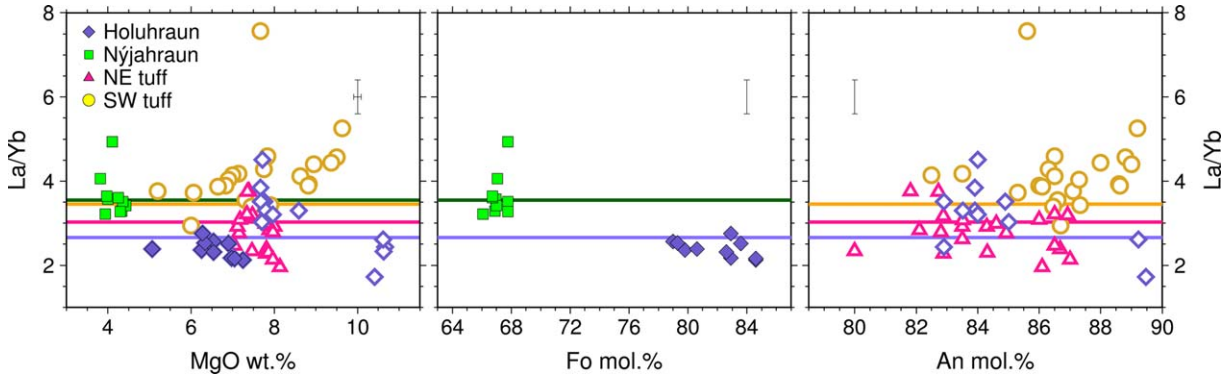

Figure 10. La/Yb variation in melt inclusions from the Askja volcanic system as a function of melt inclusion composition and host mineral composition. Olivine-hosted melt inclusions shown by coloured symbols; plagioclase-hosted melt inclusions shown by open symbols. Solid lines show the average La/Yb of glass from each eruption. The modal La/Yb ratios of melt inclusions from Nýjahraun and the NE tuff cone correspond to the average La/Yb of the glasses from these eruptions. The modal La/Yb of melt inclusions from the SW tuff cone is higher than the average La/Yb of matrix glasses from the SW tuff cone. The modal La/Yb of melt inclusions from Holuhraun is lower than the average Holuhraun glass composition. A cluster of Holuhraun melt inclusions at ~7.7 wt.% MgO have significantly higher La/Yb than the glass, and may represent an enriched magma that subsequently mixed with the Holuhraun magma. See text for details.

from the SW tuff cone show a much wider range in La/Yb than the other eruptions, and the whole-rock La/Yb is lower than the melt inclusion average La/Yb (Figure 10c). This indicates that the melt inclusions from the SW tuff cone may not share a genetic relationship with their carrier melt, but may instead be hosted in xenocrysts entrained in the carrier melt from an unrelated melt batch or mush horizon.

[48] Most Holuhraun melt inclusions have La/Yb ratios that are very similar to the Holuhraun glass. However, a small cluster of plagioclase-hosted inclusions with ~7.7 wt.% MgO have higher La/Yb than the average glass composition (Figure 10). These melt inclusions are all hosted in An_{83} plagioclase crystals from the Holuhraun-1 lava. It is possible that these high-La/Yb melt inclusions preserve some of the compositional diversity of melts being supplied to Holuhraun, and crystallized from a more enriched melt composition before it was mixed into the Holuhraun magma. Alternatively, these melt inclusions may be hosted in xenocrystic plagioclases. Without additional compositional data, it is difficult to evaluate which of these hypotheses is correct.

9. Nb-Zr-Y Systematics in Whole-Rock and Melt Inclusions

[49] A number of recent studies have utilized Nb-Zr-Y systematics to investigate the composition of the mantle source supplying melt beneath Iceland [e.g., *Fitton et al.*, 1997; *Hardarson et al.*, 1997; *Kempton et al.*, 2000; *Fitton et al.*, 2003]. Nb/Zr is insensitive to fractional crystallization, crustal contamination and subsequent alteration; thus, the Nb/Zr of moderately evolved basalts (MgO>5 wt.%) reflects an average of melts derived from the mantle, and at high MgO (>10 wt.%), Nb/Zr may be used as a proxy for source enrichment [*Shorttle and Maclennan*, 2011].

[50] Nb/Zr ratios allow whole-rock samples in this study to be refined into three separate trends (Figure 11a). Nýjahraun, Fjárhólahraun and the Askja 20th century basalts have an average Nb/Zr of 0.116 ± 0.001 (1σ), and are compositionally indistinguishable from one another in terms of their whole-rock Nb/Zr. The two Askja tuff cones have a slightly lower average Nb/Zr of 0.108 ± 0.001. Samples from Holuhraun are noticeably offset from these two trends with a much lower Nb/Zr of 0.093 ± 0.001, indicative of a more depleted mantle source composition.

[51] Melt inclusions from Holuhraun and the Askja NE tuff cone are almost indistinguishable in Nb/Zr within analytical uncertainty (Figure 11b). For both these eruptions and for Nýjahraun, the average Nb/Zr of the melt inclusions is almost identical to the average Nb/Zr of the matrix glasses (Figures 11b and 11c), indicating that the melt inclusions share a genetic relationship with their carrier melts. This is not the case for the SW

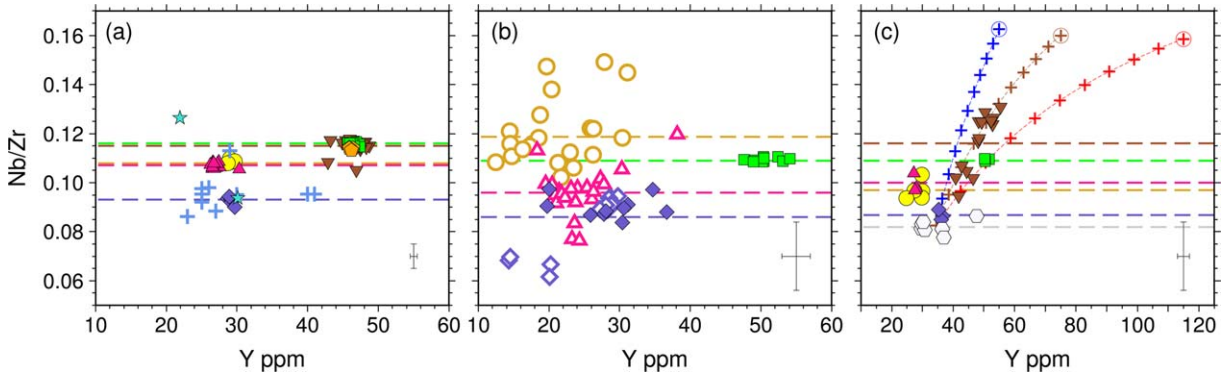

Figure 11. Variations in Nb/Zr for samples from the Askja volcanic system. Basalts from the Veiðivötn volcanic system [*Hémond et al*., 1993; *Zellmer et al*., 2008, and new samples from this study] are shown by blue crosses; other eruptions are shown using same symbols as Figure 4. The coloured dashed lines show the average Nb/Zr for each eruption: dark blue, Holuhraun; green, Nýjahraun; pink, NE tuff cone; yellow, SW tuff cone; brown, Askja 20th century basalts; gray, 1875 precursors. The error bars show 1σ precision estimates based on repeat analyses of standards. (a) Whole-rock variations in Nb/Zr versus Y, analyzed by XRF. The Veiðivötn samples have almost identical Nb/Zr values to Holuhraun (dark blue diamonds). (b) Melt inclusions, analyzed by SIMS. Olivine-hosted melt inclusions shown by coloured symbols; plagioclase-hosted melt inclusions shown by open symbols. (c) Glasses, analyzed by SIMS. All the samples except the Askja 20th century basalts plot on subparallel trends with approximately constant Nb/Zr. The range in Nb/Zr within the Askja 20th century basalts may be explained by mixing with evolved contaminant melts. Potential contaminant compositions are Icelanditic pumices (blue) and leucocratic xenoliths (red), both of which are found within the 28–29 March 1875 rhyolitic tephra deposits [*Macdonald et al*., 1987]. A hypothetical contaminant (brown) containing 48 ppm Nb, 300 ppm Zr and 75 ppm Y provides a good fit to the data. The three mixing trends shown use the average pre-1875 tephra composition as the more primitive endmember. Crosses indicate intervals of 10% mixing.

tuff cone, where the melt inclusions have a much higher average Nb/Zr than the matrix glasses. This is consistent with the observations made in section 8 that many of the SW melt inclusions are likely to be xenocryst-hosted.

[52] Glasses from Nýjahraun have higher Nb/Zr than glasses from the pre-1875 tephra samples (Figure 11c). This difference in Nb/Zr is retained even for high Zr >170 ppm, and cannot be produced by fractional crystallization. This indicates that the Nýjahraun carrier melt had a more enriched composition than the basaltic magma upwelling beneath Askja in early 1875; thus, the Nýjahraun eruptions could not have been fed by the lateral injection of magma with the "pre-1875" composition from Askja into the fissure swarm.

[53] Glasses from the Askja 20th century eruptions show significant variability in Nb/Zr ($0.095<Nb/Zr<0.131$; Figure 11c). These glasses appear to define a trend that cross-cuts the lines of constant Nb/Zr defined by glasses from Holuhraun, Nýjahraun and the Askja tuff cones. This trend cannot be produced by fractional crystallization. It is possible to describe the Askja 20th century glasses in terms of mixing a more primitive basaltic melt with evolved contaminants. Potential contaminant compositions include the "X2" leuoratic xenoliths and icelanditic pumices that are found in rhyolitic tephra from the 28–29 March 1875 eruption [*Macdonald et al*., 1987], both of which have high Nb/Zr. Mixing trends between these evolved compositions and the average composition of the pre-1875 tephra are shown in Figure 11c. While the two mixing trends bracket the Askja 20th century glass compositions, neither provides a precise fit to the data. An excellent fit to the Askja 20th century glass compositions can be achieved by up to 50% mixing with a hypothetical contaminant containing 48 ppm Nb, 300 ppm Zr, and 75 ppm Y (Figure 11c); however, we note that no erupted products with this composition have yet been found at Askja.

[54] The Nýjahraun glasses appear to fall on the mixing trend between the pre-1875 basaltic tephra and the X2 xenoliths (Figure 11c). However, the Nýjahraun melt inclusions and glasses are homogeneous in Nb/Zr. If Nýjahraun and the Askja 20th

century basalts are assumed to have originated from a common magma source and thus to have mixed with the same evolved contaminants in a shallow magma chamber, then Nýjhraun would be expected to show the same degree of Nb/Zr variability as the Askja 20th century basalts. The fact that this is not observed leads us to suggest that, while the magma supplying the Askja 20th century basalts mixed with an evolved contaminant and/or assimilated partial melts of basaltic crustal material, the Nýjahraun carrier melt evolved without such interactions. This carries the implication that the carrier melts for Nýjahraun and the Askja 20th century basalts did not share a common magmatic origin.

[55] A striking feature of the whole-rock Nb-Zr-Y systematics is that Holuhraun and Tröllahraun whole-rock samples are chemically similar to lavas from the Veiðivötn volcanic system. The Veiðivötn compositional data shown in Figure 11 include published analyses of lavas from the Veiðivötn volcanic system [*Hémond et al*., 1993; *Zellmer et al*., 2008], plus samples from the Thjórsá lava, two lava flows from Thjórsárdalur valley, and samples from the Brandur and Fontur tuff cones, analyzed by XRF at the University of Edinburgh. Although there is some scatter in the Veiðivötn data, the samples considered have an average Nb/Zr of 0.096 ± 0.007, which is similar to the Holuhraun whole-rock. The Holuhraun lava is thus compositionally more similar to basalts from the Veiðivötn than to basalts from Askja, despite the fact that Holuhraun is geographically situated within the Askja volcanic system.

10. Discussion

10.1. Implications for the Lateral Flow Hypothesis

[56] Whilst the whole-rock major element compositions of Nýjahraun and the Askja 20th century basalts are broadly similar, they differ in certain whole-rock trace element ratios (e.g., Zr/Ni, Figure 4d), and can also be distinguished by compositional differences in the major and trace element geochemistry of their matrix glasses (Figures 5 and 6). These eruptions are also petrologically different: Nýjahraun contains abundant olivine, plagioclase and clinopyroxene phenocrysts (Figure 3), while the Askja 20th century basalts are essentially aphyric. Taken together, the differences suggest that these magmas did not share a common parental magma, and have different magmatic histories. It is therefore difficult to explain the Nýjahraun fissure eruptions in terms of northward lateral transport of magma from Askja. Thus, our results lend support to the magma reservoir hypothesis, whereby eruptions on the fissure swarm are fed by vertical magma flow.

[57] Both whole-rock and glass compositons from Fjárhólahraun bear a strong compositional similarity to those of the Askja 20th century basalts (Figures 4, 5, 6, and 11a). It is therefore possible that the Fjárhólahraun magma shared a common source with the Askja 20th century basalts. If Fjárhólahraun was erupted during the 1874–1876 volcano-tectonic episode, and was fed from a magma reservoir beneath Askja, this would imply that lateral magma injections extended up to 15 km north of Askja central volcano. It is also notable that the Thorvaldshraun fissure lava of 1924–1929, on Askja's southern flanks, is compositionally identical to the basalts erupted within Askja caldera during the early 20th century, which suggests that all the Askja 20th century basalts, including Thorvaldshraun, were sourced from a common magma batch resident in Askja's shallow crustal magma chamber. The Thorvaldshraun fissures are sufficiently close to Askja that inclined to subvertical injections of magma from Askja are most likely to have fed this eruption. Our data therefore indicate that lateral dyke injection may be a mechanism that supplies magma to fissure eruptions in the near vicinity of Askja central volcano.

[58] Holuhraun is compositionally very different to any of the samples from Askja or farther north on the Askja volcanic system. This is evident from major and trace element concentrations in both whole-rock and glass compositions, and demonstrates that Holuhraun cannot have been sourced by lateral flow southward from Askja. The compositional similarity of Holuhraun magmas with those from Tröllahraun suggests that Holuhraun may bear more resemblance to magmas erupted on the Veiðivötn volcanic system than to those of the Askja volcanic system. If Holuhraun and Tröllahraun erupted during a single volcano-tectonic episode that caused rifting on the northern and western margins of Vatnajökull, then the eruption of Holuhraun is entirely unrelated to the 1874–1876 Askja volcano-tectonic episode.

[59] Although the Askja 1874–1876 volcano-tectonic episode is often compared with the 1975–1984 Krafla Fires [e.g., *Björnsson et al*., 1977; *Tryggvason*, 1984], it is difficult to compare these

events directly, since fissure eruptions at Askja occurred 45–60 km from the central volcano, while the most northerly eruptive fissure during the Krafla Fires extended just 6 km from the Krafla caldera [*Einarsson*, 1991]. It is true that northward-propagating earthquake swarms during the Krafla Fires did extend up to 65 km north of Krafla caldera [*Tryggvason*, 1984]. However, we suggest that these earthquakes should not necessarily be interpreted as synonymous with lateral magma injection [e.g., *Einarsson and Brandsdóttir*, 1979], since it is also possible that the propagation of tensile failure in the rift zone opened a fracture [e.g., *Gudmundsson*, 1995], but that magma flow within this fracture was primarily vertical. The absence of seismic records for the Askja 1874–1876 volcano-tectonic episode also hinders direct comparison with rifting events observed at mid-ocean ridges [e.g., *Dziak et al*., 2004] or in Afar [e.g., *Ayele et al*., 2009, and references therein]. While the rifting in Afar resulted in two basaltic eruptions from a fissure ~6–12 km southeast of Dabbahu volcano in August 2007 and June 2009 [*Ferguson et al*., 2010], there was no contemporaneous eruption at Dabbahu itself [*Field et al*., 2012]. A geochemical investigation of these basalts and their relationship (or lack thereof) to rhyolitic ash erupted from the Da'Ure vent, ~7 km ENE of Dabbahu summit, in September 2005 [*Ayele et al*., 2007] would provide an interesting comparison with the Askja 1874–1876 volcano-tectonic episode.

10.2. Implications for the Delineation of Volcanic Systems

[60] Major element compositions and ratios in Icelandic basalts have proved to be a convenient and reliable way to identify and discriminate between samples from different volcanic systems, and to assign tephras to their source volcano [e.g., *Jakobsson*, 1979; *Larsen and Eiríksson*, 2008; *Jagan*, 2010; *Óladóttir et al*., 2011]. Basalts from the Veiðivötn volcanic system can be distinguished from those of Askja by their lower K_2O concentrations and lower TiO_2/FeO [*Jagan*, 2010]. For a given TiO_2/FeO, glasses from Holuhraun and Tröllahraun have lower K_2O than basalts from the Askja tuff cones (Figure 6), and match the "Veiðivötn" group better than they match compositions from Askja. Holuhraun and Tröllahraun whole-rock samples also have similar Nb/Zr to whole-rock samples from around the Veiðivötn volcanic system (Figure 11), but lower Nb/Zr than samples from Askja central volcano. Additional similarities between Veiðivötn lava samples and Holuhraun are apparent on the macro-scale: Veiðivötn lavas and tuffs are often characterized by the type of glomerocrystic crystal clots that have been found in Holuhraun [*Hanan et al*., 2000; *Halldorsson et al*., 2008], while postglacial lavas from the Askja volcanic system are normally very phenocryst-poor [*Hartley*, 2012].

[61] Implicit in the practice of identifying the source volcanic system of an unknown basaltic sample on a geochemical basis is the idea that individual volcanic systems bear unique and statistically significant geochemical characteristics that will be present in all erupted products from that volcanic system. Icelandic volcanic systems are traditionally defined by their surface expressions—that is, by the locations of normal faults and grabens in the brittle crust that delineate zones of active extension. Cone rows and volcanic fissures generally fall within a specific volcanic system, since ascending melts will exploit existing faults, and will tend to flow in a direction perpendicular to the direction of spreading during rifting episodes [e.g., *Gudmundsson*, 1984, 1995, 2006]. Thus, fissure eruptions are said to "belong" to the volcanic system within whose surface expression they fall, although it is difficult to apply this method to subglacial eruptions when the surface expressions of volcanic systems are obscured [*Gudmundsson and Högnadóttir*, 2007].

[62] According to existing tectonic maps of Iceland [*Jóhannesson and Sæmundsson*, 1998], the Holuhraun fissure is part of the Askja volcanic system. However, this is not consistent with our geochemical data, which suggest that Holuhraun is geochemically most similar to the Veiðivötn volcanic system. This apparent anomaly suggests that our understanding of the link between geochemistry and the surface expression of Icelandic volcanic systems may be overly simplistic. If volcanic systems are defined by their surface expressions, then geochemical characteristics may not necessarily be unique to individual volcanic systems. However, if volcanic systems are defined by unique and distinctive geochemical signatures, then the present identification and delineation of the boundaries between volcanic systems beneath the north-west sector of Vatnajökull is in need of further consideration.

[63] Although Icelandic volcanic systems may be delineated by the locations of normal faults and grabens in the brittle crust, the melt generation region is decoupled from the upper crust. That is, the location of melt generation in the mantle is not

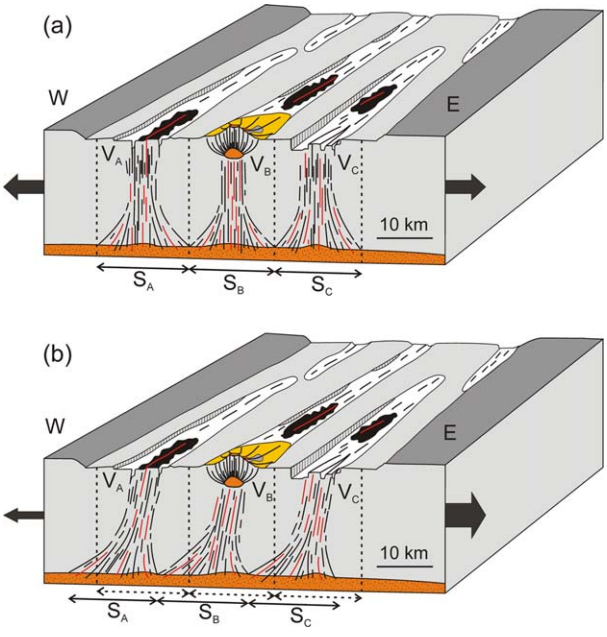

Figure 12. Schematic diagram of magma supply to volcanic systems in North Iceland, modified after *Gudmundsson* [1987b]. The vertical axis is not to scale. (a) Volcanic systems aligned perpendicular to the direction of spreading. Melts generated in the lower crust are channelled into particular volcanic systems on the basis of their location, i.e., melts generated in source region B (S_B) will be channelled into, and erupt along, volcanic system B (V_B). Melts generated at the midpoint between V_A and V_B, which is the midpoint of the surface expressions of collinear volcanic systems A and B, may be channelled into either volcanic system with equal probability. (b) Rotation of volcanic systems with respect to the spreading direction, and/or slightly asymmetric plate spreading, may cause the shearing of melt supply to collinear volcanic systems. The surface expressions of volcanic systems A, B, and C remain fixed, but the source regions supplying melts to these systems are sheared to the west. This provides a mechanism whereby melt compositions normally associated with volcanic system A may be channelled into volcanic system B, as may be the case for Veiðivötn and Askja.

determined by brittle features in the upper crust. Once a melt has been transported from its source region to the brittle crust, it is constrained to erupt within a particular volcanic system. However, melt transport pathways through the ductile lower crust cannot be constrained by examining features in the brittle upper crust. Thus, a melt should not be considered to belong to a particular volcanic system until it has reached the brittle-ductile transition in the crust. This is of particular importance for closely spaced, collinear volcanic systems such as Askja and Veiðivötn. In an ideal model where volcanic systems are exactly perpendicular to the direction of spreading, and the spreading rates are equal on either side of the volcanic system, then the location of melt generation will determine which volcanic system a melt is channelled into by virtue of buoyant magma upwelling (Figure 12a). Melts generated at the exact midpoint of the surface expressions of two volcanic systems have an equal probability of eruption on either volcanic system, since no external stresses favour the channelling of melt toward either volcanic system. However, melt generated at the midpoint of two volcanic systems will almost certainly mix with other melt batches generated within the boundaries of a single volcanic system prior to its eruption. Therefore, under symmetric spreading rates, any defining geochemical characteristics of a volcanic system are preserved.

[64] The association of geochemical characteristics with a particular volcanic system may be destroyed if there is a change in the tectonic stresses, producing asymmetrical half-spreading rates or causing the rotation of volcanic systems such that they are no longer orientated perpendicular to the direction of spreading. Changes in tectonic stress may affect the way magmas are channelled from the melt source region into the brittle crust (Figure 12b), while rotations of volcanic systems allow one volcanic system to tap melts that, under conditions of symmetric stress, would have been channelled into the adjacent volcanic system. There is abundant evidence for rotational shear stresses in the Askja region. The fissure swarm has a strike of ~20° on the Eastern Volcanic Zone south of Askja, but strikes at ~5° on the Northern Volcanic Zone in North Iceland. At Askja itself, two sets of fissures and lineaments striking between 5 and 20° are cross cut by a transform fault swarm striking 300° [*Sigvaldason*, 2002]. Numerous east-west trending volcanic lineaments, cone rows and fissures are also found in the region south of Askja [*Hjartardóttir et al.*, 2009; *Hartley and Thordarson*, 2012]. It is therefore possible that rotational stresses provide a mechanism whereby melts with compositions more commonly associated with the Veiðivötn volcanic system may be channelled and transported eastward into what is traditionally delineated as part of the Askja volcanic system.

[65] In light of our new geochemical data, we suggest that the Veiðivötn volcanic system may extend beneath the north-west corner of Vatnajökull toward Dyngjujökull and the region south of Askja (see supplementary information, Figure S3). A similar idea was proposed by *Larsen* [1982]; however, Larsen linked the Veiðivötn volcanic

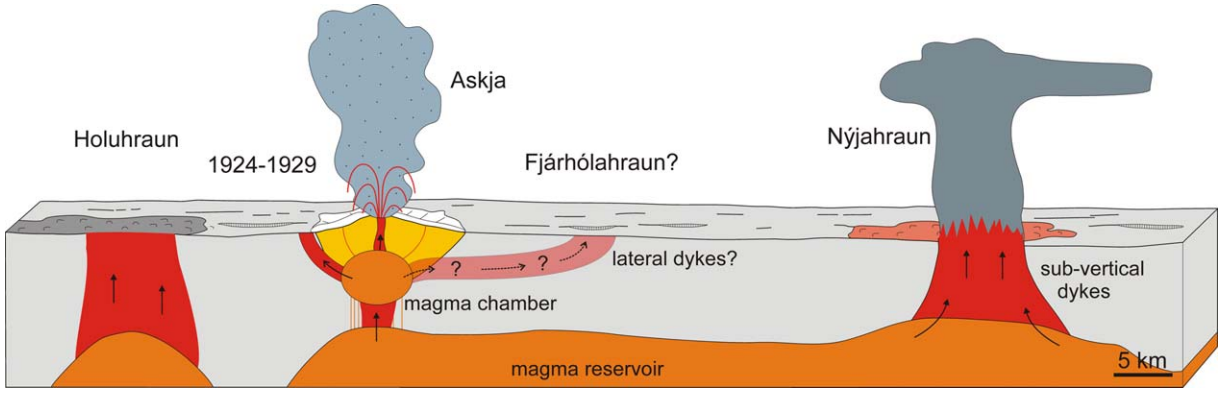

Figure 13. Schematic diagram summarizing the events of the 1874–1876 Askja volcano-tectonic episode. Magmas erupted at Askja and Nýjahraun during this episode evolved independently of each other in separate magma storage regions and arrived at the surface via separate plumbing systems. The Askja 20th century basalts are thought to have mixed with evolved melts in the crust while the Nýjahraun magma evolved without such interactions. It is likely that lateral or oblique magma flow from Askja fed the Fjárhólahraun and Thorvaldshraun eruptions. The Holuhraun fissure eruptions were unrelated to the 1874–1876 volcano-tectonic episode, and had an entirely separate magma plumbing system.

system across the Dyngjuháls region immediately north of Vatnajökull, and extended it northward across the Trölladyngja region, west of Askja central volcano. By placing the boundary between the Bárðarbunga-Veiðivötn and Askja volcanic systems to the west of Askja, *Larsen* [1982] assumed that Holuhraun and other lavas to the south of Askja were associated with Askja. However, the data presented in this study show that this is not the case: Holuhraun is geochemically more similar to Veiðivötn basalts. The geochemical boundary between Askja and Veiðivötn must therefore lie in the region immediately to the south of Askja, with fissures extending northward from Dyngjujökull having "Veiðivötn"-like compositions, but fissures extending southward from Askja having "Askja"-like compositions. This may result in some interfingering at the intersection where magmas from the two systems cut into one another, in a similar manner to that reported between the Veiðivötn and Torfajökull volcanic systems in southeast Iceland [*McGarvie*, 1984; *Mørk*, 1984; *Macdonald et al*., 1990; *McGarvie et al*., 1990; *Zellmer et al*., 2008]. However, we have not found evidence of Holuhraun having mingled or mixed with Askja-derived magmas, while magma mingling is evident in the Veiðivötn and Torfajökull case. It is possible that the geochemical boundary between Veiðivötn and Askja could be further constrained using radiogenic isotope data, which have proved particularly useful in in distinguishing between the products of neighbouring volcanic systems [e.g., *Sigmarsson et al*., 2000].

11. Conclusions

[66] New geochemical data suggest that magmas erupted at Askja and Nýjahraun during the 1874–1876 volcano-tectonic episode evolved independently of each other in separate magma storage regions and arrived at the surface via separate plumbing systems. Although the Askja and Nýjahraun magmas are geochemically similar in whole-rock major and trace element compositions, the Askja 20th century basalts are thought to have evolved via mixing with evolved melts in the crust, while the Nýjahraun magma evolved without such interactions. The Holuhraun fissure eruptions had an entirely separate magma plumbing system and were not connected with the 1874–1876 volcano-tectonic episode.

[67] Our preferred interpretation of the events of the 1874–1876 volcano-tectonic episode is summarized in Figure 13. The 1874–1876 volcano-tectonic episode activated an ~80 km long segment of the Askja volcanic system. Magma upwelled from an elongate reservoir at the base of the crust, with upwelling focused beneath Askja and the Sveinagjá graben, 45–65 km north of Askja. The upwelling of hot, primitive magma beneath Sveinagjá initiated the eruption of an evolved basaltic magma that had resided in a shallow crustal melt lens beneath Sveinagjá, but had not assimilated crustal material. Upwelling at the central volcano initiated convective overturn in a large, stratified shallow crustal magma chamber.

Evolved basaltic magma from the stratified magma chamber was probably injected northward into the fissure swarm, resulting in a fissure eruption at Fjárhólar. Minor precursory activity at Askja in early January 1875 included the eruption of a basaltic tephra with composition similar to that of two phreatomagmatic tuff cone sequences in the Askja caldera. The precursory eruptions were followed by an explosive, Plinian eruption on 28–29 March 1875 that generated 0.321 km^3 of rhyolitic tephra [*Carey et al*., 2010] and initiated the collapse of Öskjuvatn caldera. In the early 20th century, after 40 years of continued caldera collapse events [*Hartley and Thordarson*, 2012], evolved basalt from Askja's shallow magma chamber was erupted along the Öskjuvatn caldera ring fractures and injected southward into the fissure swarm, causing a fissure eruption on Askja's southern flanks. These magmas had mixed with minor amounts of an evolved contaminant. The Holuhraun fissure eruption was unconnected with the 1874–1876 Askja volcano-tectonic episode, and is compositionally unlike magmas from the Askja volcanic system. Its compositional similarity to the Tröllahraun lava, erupted between 1862 and 1864 on the Veiðivötn volcanic system, suggests that Holuhraun may also have erupted in the 1860s. The discovery of magma with Veiðivötn-like macroscopic and geochemical characteristics on what is traditionally thought to be part of the Askja volcanic system has important implications for the identification and delineation of fissure systems beneath the north-east sector of Vatnajökull.

Acknowledgments

[68] We thank Cees-Jan de Hoog, Chris Hayward, Nic Odling and Valérie Olive for their help with the SIMS, EPMA, XRF and ICP-MS analyses respectively. Guðrun Larsen, Ben Winpenny, David Neave and Alexandra de Joux assisted with various aspects of the field work. We are grateful to Oli Shorttle for allowing us to use unpublished analyses of Tröllahraun tephra. Thorough and constructive reviews from John Sinton and two anonymous reviewers improved and clarified the manuscript. Access to the Edinburgh Ion Microprobe Facility was funded by NERC grant IMF386/1109. MEH was supported by NERC studentship NE/F008929/1.

References

Ariskin, A. A., M. Y. Frenkel, G. S. Barmina, and R. L. Nielsen (1993), COMAGMAT: A Fortran program to model magma differentiation processes, *Comput. Geosci.*, *19*, 1155–1170.

Ayele, A., E. Jacques, M. Kassim, T. Kidane, A. Omar, S. Tait, A. Nercessian, J. B. de Chabalier, and G. King (2007), The volcano-seismic crisis in Afar, Ethiopia, starting September 2005, *Earth Planet. Sci. Lett.*, *255*(1–2), 177–187.

Ayele, A., D. Keir, C. Ebinger, T. J. Wright, G. W. Stuart, W. R. Buck, E. Jacques, G. Ogubazghi, and J. Sholan (2009), September 2005 mega-dike emplacement in the Manda-Harraro nascent oceanic rift (Afar depression), *Geophys. Res. Lett.*, *36*, L20306, doi:10.1029/2009GL039605.

Bárðarson, G. G. (1929), Geologisk kort over Reykjanes-Halvøen, *Skand. Naturforskermøde*, *18*, 182–190.

Björnsson, A., K. Sæmundsson, P. Einarsson, E. Tryggvason, and K. Grönvold (1977), Current rifting episode in north Iceland, *Nature*, *266*(5600), 318–323.

Brandsdóttir, B. (1992), Historical accounts of earthquake associated with eruptive activity in the Askja volcanic system, *Jökull*, *42*, 1–9.

Buck, W. R., P. Einarsson, and B. Brandsdóttir (2006), Tectonic stress and magma chamber size as controls on dike propagation: Constraints from the 1975–1984 Krafla rifting episode, *J. Geophys. Res.*, *111*, B12404, doi:10.1029/2005JB003879.

Carey, R. J., B. F. Houghton, and T. Thordarson (2010), Tephra dispersal and eruption dynamics of wet and dry phases of the 1875 eruption of Askja Volcano, Iceland, *Bull. Volcanol.*, *72*, 259–278.

Danyushevsky, L. V., and P. Plechov (2011), Petrolog3: Integrated software for modeling crystallization processes, *Geochem. Geophys. Geosyst.*, *12*, Q07021, doi:10.1029/2011GC003516.

Dziak, R. P., C. G. Fox, and A. E. Schreiner (1995), The June-July 1993 seismo-acoustic event at CoAxial segment, Juan de Fuca Ridge: Evidence for a lateral dike injection, *Geophys. Res. Lett.*, *22*(2), 135–138.

Dziak, R. P., D. K. Smith, D. R. Bohnenstiehl, C. G. Fox, D. Desbruyeres, H. Matsumoto, M. Tolstoy, and D. J. Fornari (2004), Evidence of a recent magma dike intrusion at the slow spreading Lucky Strike segment, Mid-Atlantic Ridge, *J. Geophys. Res.*, *109*, B12102, doi:10.1029/2004JB003141.

Ebinger, C. J., D. Keir, A. Ayele, E. Calais, T. J. Wright, M. Belachew, J. O. S. Hammond, E. Campbell, and W. R. Buck (2008), Capturing magma intrusion and faulting processes during continental rupture: Seismicity of the Dabbahu (Afar) rift, *Geophys. J. Int.*, *174*(3), 1138–1152.

Einarsson, P. (1991), Earthquakes and present-day tectonism in Iceland, *Tectonophysics*, *189*(1–4), 261–279.

Einarsson, P., and B. Brandsdóttir (1979), Seismological evidence for lateral magma intrusion during the July 1978 deflation of the Krafla volcano in NE-Iceland, *Nordic Volcanol. Inst.*, *79*(9), 1–14.

Einarsson, P., and K. Sæmundsson (1987), Earthquake epicenters 1982–1985 and volcanic systems in Iceland (map), in *Í hlutarins edli: Festschrift for Thorbjörn Sigurgeirsson*, edited by T. Sigfússon, Menningarsjóður, Reykjavík.

Ferguson, D. J., T. D. Barnie, D. M. Pyle, C. Oppenheimer, G. Yirgu, E. Lewi, T. Kidane, S. Carn, and I. Hamling (2010), Recent rift-related volcanism in Afar, Ethiopia, *Earth Planet. Sci. Lett.*, *292*, 409–418.

Fialko, Y. A., and A. M. Rubin (1998), Thermodynamics of lateral dike propagation: Implications for crustal accretion at slow spreading mid-ocean ridges, *J. Geophys. Res.*, *103*, 2501–2514.

Field, L., T. Barnie, J. Blundy, R. A. Brooker, D. Keir, E. Lewi, and K. Saunders (2012), Integrated field, satellite and petrological observations of the November 2010 eruption of Erta Ale, *Bull. Volcanol.*, *74*, 2251–2271.

Fitton, J. G., and M. Godard (2004), Origin and evolution of magmas on the Ontong Java Plateau, *Geol. Soc. London Spec. Publ.*, *229*, 151–178.

Fitton, J. G., A. D. Saunders, M. J. Norry, B. S. Hardarson, and R. N. Taylor (1997), Thermal and chemical structure of the Iceland plume, *Earth Planet. Sci. Lett.*, *153*(3–4), 197–208.

Fitton, J. G., A. D. Saunders, L. M. Larsen, B. S. Hardarson, and M. J. Norry (1998), Volcanic rocks from the southeast Greenland margin at 63° N: Composition, petrogenesis and mantle sources, *Proc. Ocean Drill. Prog. Sci. Results*, *152*, 331–350.

Fitton, J. G., A. D. Saunders, P. D. Kempton, and B. S. Hardarson (2003), Does depleted mantle form an intrinsic part of the Iceland plume? *Geochem. Geophys. Geosyst.*, *4*(3), 1032, doi:10.1029/2002GC000424.

Ford, C. E., D. G. Russell, J. A. Craven, and M. R. Fisk (1983), Olivine-liquid equilibria: temperature, pressure and composition dependence of the crystal/liquid cation partition coefficients for Mg, Fe^{2+}, Ca and Mn, *J. Petrol.*, *24*(3), 256–266.

Grove, T. L., R. J. Kinzler, and W. B. Bryan (1992), Fractionation of mid-ocean ridge basalt (MORB), *Geophys. Monogr.*, *71*, 281–310.

Gudmundsson, A. (1984), Formation of dykes, feeder-dykes, and the intrusion of dykes from magma chambers, *Bull. Volcanol.*, *47*(3), 537–550.

Gudmundsson, A. (1987a), Lateral magma flow, caldera collapse, and a mechanism of large eruptions in Iceland, *J. Volcanol. Geotherm. Res.*, *34*, 65–78.

Gudmundsson, A. (1987b), Formation and mechanics of magma reservoirs in Iceland, *Geophys. J. R. Astron. Soc.*, *91*, 27–41.

Gudmundsson, A. (1995), Infrastructure and mechanics of volcanic systems in Iceland, *J. Volcanol. Geotherm. Res.*, *64*, 1–22.

Gudmundsson, A. (2006), How local stresses control magma-chamber ruptures, dyke injections, and eruptions in composite volcanoes, *Earth Sci. Rev.*, *79*, 1–31.

Gudmundsson, M. T., and T. Högnadóttir (2007), Volcanic systems and calderas in the Vatnajökull region, central Iceland: Constraints on crustal structure from gravity data, *J. Geodyn.*, *43*(1), 153–169.

Guðmundsson, F. (1932), Endurminningar (Memoirs)—Dyngjufjallagosið, pp. 26–29, Viking, Winnipeg.

Gunnarsson, S. (1875), Vikuröskufall í Múlasýslum á 2. í páskum, 29 marz, 1875 (Pumice fall in the Múlasýslur, 2nd day of Easter, 29 March, 1875). Letter written on 24 April 1875, *Norðanfari*, *14*(27–28), 58–59.

Halldorsson, S. A., N. Óskarsson, K. Grönvold, G. Sigurdsson, G. Sverrisdóttir, and S. Steinthórsson (2008), Isotopic-heterogeneity of the Thjorsa lava: Implications for mantle sources and crustal processes within the Eastern Rift Zone, Iceland, *Chem. Geol.*, *255*(3–4), 305–316.

Hanan, B. B., J. Blichert-Toft, R. Kingsley, and J.-G. Schilling (2000), Depleted Iceland mantle plume geochemical signature: Artifact of multicomponent mixing? *Geochem. Geophys. Geosyst.*, *1*(4), 1003, doi:10.1029/1999GC000009.

Hansen, H., and K. Grönvold (2000), Plagioclase ultraphyric basalts in Iceland: The mush of the rift, *J. Volcanol. Geotherm. Res.*, *98*(1–4), 1–32.

Hardarson, B. S., J. G. Fitton, R. M. Ellam, and M. S. Pringle (1997), Rift relocation - A geochemical and geochronological investigation of a palaeo-rift in northwest Iceland, *Earth Planet. Sci. Lett.*, *153*(3–4), 181–196.

Hartley, M. E. (2012), Postglacial volcanism and magmatism on the Askja volcanic system, North Iceland, PhD thesis, Univ. of Edinburgh, Edinburgh, U. K.

Hartley, M. E., and T. Thordarson (2012), Formation of Öskjuvatn caldera at Askja, North Iceland: Mechanism of caldera collapse and implications for the lateral flow hypothesis, *J. Volcanol. Geotherm. Res.*, *227-228*, 85–101.

Hartley, M. E., T. Thordarson, C. Taylor, J. G. Fitton, and EIMF (2012), Evaluation of the effects of composition on instrumental mass fractionation during SIMS oxygen isotope analyses of glasses, *Chem. Geol.*, *334*, 312–323.

Hayward, C. L. (2012), High spatial resolution electron probe microanalysis of tephras and melt inclusions without beam-induced chemical modification, *Holocene*, *22*, 119–125, doi:10.1177/0959683611409777.

Hémond, C., N. T. Arndt, U. Lichtenstein, A. W. Hofmann, N. Óskarsson, and S. Steinthórsson (1993), The heterogeneous Iceland plume: Nd-Sr-O isotopes and trace element constraints, *J. Geophys. Res.*, *98*(B9), 15,833–15,850, doi:10.1029/93JB01093.

Hjartardóttir, Á. R., P. Einarsson, and H. Sigurdsson (2009), The fissure swarm of the Askja volcanic system along the divergent plate boundary of N Iceland, *Bull. Volcanol.*, *71*(9), 961–975.

Jagan, A. (2010), Tephra stratigraphy and geochemistry from three Icelandic lake cores: A new method for determining source volcano of tephra layers, Master's thesis, Univ. of Edinburgh, Edinburgh, U. K.

Jakobsson, S. P. (1979), Petrology of recent basalts of the Eastern Volcanic Zone, Iceland, *Acta Natur. Islandica*, *26*, 1–103.

Jóhannesson, H., and K. Sæmundsson (1998), Geological Map of Iceland, 1:600,000, Bedrock Geology, Icelandic Inst. of Nat. Hist., Reykjavík.

Jónsson, O. (1945), *Ódáðahraun I-III*, 1276 pp., Bókaútgáfan Norðri, Akureyri.

Keir, D., et al. (2009), Evidence for focused magmatic accretion at segment centers from lateral dike injections captured beneath the Red Sea rift in Afar, *Geology*, *37*(1), 59.

Kempton, P. D., J. G. Fitton, A. D. Saunders, G. M. Nowell, R. N. Taylor, B. S. Hardarson, and G. Pearson (2000), The Iceland plume in space and time: A Sr-Nd-Pb-Hf study of the North Atlantic rifted margin, *Earth Planet. Sci. Lett.*, *177*, 255–271.

Larsen, G. (1982), Gjóskutímatal Jökuldals og nágrennis (Tephrochronology of the Jökuldalur area and its vicinity), in *Eldur er í Norðri*, edited by H. Thórarinsdóttir, et al., pp. 51–65, Sögufélag, Reykjavík.

Larsen, G., and J. Eiríksson (2008), Holocene tephra archives and tephrochronology in Iceland: A brief overview, *Jökull*, *58*, 229–250.

Larsen, G., and S. Thorarinsson (1977), H4 and other acid Hekla tephra layers, *Jökull*, *27*, 28–46.

Macdonald, R., R. S. J. Sparks, H. Sigurðsson, D. P. Mattey, D. W. McGarvie, and R. L. Smith (1987), The 1875 eruption of Askja volcano, Iceland: Combined fractional crystallisation and selective contamination in the generation of rhyolitic magma, *Mineral. Mag.*, *51*, 183–202.

Macdonald, R., D. W. McGarvie, H. Pinkerton, R. L. Smith, and A. Palacz (1990), Petrogenetic evolution of the Torfajökull Volcanic Complex, Iceland I. Relationship between the magma types, *J. Petrol.*, *31*(2), 429–459.

Maclennan, J. (2008), Concurrent mixing and cooling of melts under Iceland, *J. Petrol.*, *49*, 1931–1953.

Maclennan, J., M. Jull, D. McKenzie, L. Slater, and K. Grönvold (2002), The link between volcanism and

deglaciation in Iceland, *Geochem. Geophys. Geosyst.*, *3*(11), 1062, doi:10.1029/2001GC000282.
McGarvie, D. W. (1984), Torfajökull: A volcano dominated by magma mixing, *Geology*, *12*(11), 685–688.
McGarvie, D. W., R. Macdonald, H. Pinkerton, and R. L. Smith (1990), Petrogenetic evolution of the Torfajökull Volcanic Complex, Iceland. II. The role of magma mixing, *J. Petrol.*, *31*(2), 461–481.
Mørk, M. B. E. (1984), Magma mixing in the post-glacial Veidivötn fissure eruption, southeast Iceland: A microprobe study of mineral and glass variations, *Lithos*, *17*, 55–75.
Óladóttir, B. A., O. Sigmarsson, G. Larsen, and T. Thordarson (2008), Katla volcano, Iceland: Magma composition, dynamics and eruption frequency as recorded by Holocene tephra layers, *Bull. Volcanol.*, *70*, 475–493.
Óladóttir, B. A., O. Sigmarsson, G. Larsen, and J. L. Devidal (2011), Provenance of basaltic tephra from Vatnajökull subglacial volcanoes, Iceland, as determined by major- and trace-element analyses, *Holocene*, *21*, 1037–1048.
Olive, V., R. M. Ellam, and L. Wilson (2001), A protocol for the determination of the rare earth elements at picomole level in rocks by ICP-MS: Results on geological reference materials USGS PCC-1 and DTS-1, *Geostand. Geoanal. Res.*, *25*, 219–228.
Óskarsson, N., O. Helgason, and S. Steinthórsson (1994), Oxidation-state of iron in mantle-derived magmas of the Icelandic rift-zone, *Hyperfine Interact.*, *91*(1-4), 733–737.
Parfitt, E. A., and L. Wilson (1994), The 1983-86 Pu'u 'O'o eruption of Kilauea Volcano, Hawaii: A study of dike geometry and eruption mechanisms for a long-lived eruption, *J. Volcanol. Geotherm. Res.*, *59*(3), 179–205.
Putirka, K. (1999), Clinopyroxene plus liquid equilibria to 100 kbar and 2450 K, *Contrib. Mineral. Petrol.*, *135*(2-3), 151–163.
Putirka, K. D. (2005), Mantle potential temperatures at Hawaii, Iceland, and the mid-ocean ridge system, as inferred from olivine phenocrysts: Evidence for thermally driven mantle plumes, *Geochem. Geophys. Geosyst.*, *6*, Q05L08, doi:10.1029/2005GC000915.
Putirka, K. D. (2008), Thermometers and barometers for volcanic systems, *Rev. Mineral. Geochem.*, *69*, 61–120.
Roeder, P. L., and R. F. Emslie (1970), Olivine-liquid equilibrium, *Contrib. Mineral. Petrol.*, *29*(4), 275–289.
Ryan, M. P. (1988), The mechanics and three-dimensional internal structure of active magmatic systems: Kilauea volcano, Hawaii, *J. Geophys. Res.*, *93*(B5), 4213–4248.
Shorttle, O., and J. Maclennan (2011), Compositional trends of Icelandic basalts: Implications for short-length scale lithological heterogeneity in mantle plumes, *Geochem. Geophys. Geosyst.*, *12*, Q11008, doi:10.1029/2011GC003748.
Siebert, L., T. Simkin, and P. Kimberly (2010), *Volcanoes of the World*, 3rd ed., 551 pp., Univ. of Calif. Press, Berkeley, Calif.
Sigmarsson, O., H. R. Karlsson, and G. Larsen (2000), The 1996 and 1998 subglacial eruptions beneath the Vatnajökull ice sheet in Iceland: Contrasting geochemical and geophysical inferences on magma migration, *Bull. Volcanol.*, *61*(7), 468–476.
Sigurðsson, H., and R. S. J. Sparks (1978a), Lateral magma flow within rifted Icelandic crust, *Nature*, *274*, 126–130.
Sigurðsson, H., and R. S. J. Sparks (1978b), Rifting episode in North Iceland in 1874–1875 and the eruptions of Askja and Sveinagjá, *Bull. Volcanol.*, *41*, 149–167.
Sigurðsson, H., and R. S. J. Sparks (1981), Petrology of rhyolitic and mixed magma ejecta from the 1875 eruption of Askja, Iceland, *J. Petrol.*, *22*, 41–84.
Sigvaldason, G. E. (1979), Rifting, magmatic activity and interaction between acid and basic liquids: The 1875 Askja eruption in Iceland, *Nordic Volcanol. Inst.*, *79*(03), 1–41.
Sigvaldason, G. E. (2002), Volcanic and tectonic processes coinciding with glaciation and crustal rebound: An early Holocene rhyolitic eruption in the Dyngjufjöll volcanic centre and the formation of the Askja caldera, north Iceland, *Bull. Volcanol.*, *64*(3–4), 192–205.
Sigvaldason, G. E., H. R. Karlsson, and J. M. Browning (2002), The Askja-Sveinagja connection: Implications for the origin of low O-18 Magmas in Iceland, *AGU Fall Meet.*, Abstract V62B–1394.
Starkey, N. A., J. G. Fitton, F. M. Stuart, and L. M. Larsen (2012), Melt inclusions in olivines from early Iceland plume picrites support high $^{3}He/^{4}He$ in both enriched and depleted mantle, *Chem. Geol.*, *306*, 54–62.
Thórarinsson, S., and G. E. Sigvaldason (1972), Tröllagígar og Tröllahraun (The Tröllagígar eruption 1862–1864), *Jökull*, *22*, 12–26.
Thordarson, T., and G. Larsen (2007), Volcanism in Iceland in historical time: Volcano types, eruption styles and eruptive history, *J. Geodyn.*, *43*, 118–152.
Tryggvason, E. (1984), Widening of the Krafla fissure swarm during the 1975–1981 volcano-tectonic episode, *Bull. Volcanol.*, *47*(1), 47–69.
Wood, D. A., I. L. Gibson, and R. N. Thompson (1976), Elemental mobility during zeolite facies metamorphism of the Tertiary basalts of eastern Iceland, *Contrib. Mineral. Petrol.*, *55*(3), 241–254.
Workman, R. K., and S. R. Hart (2005), Major and trace element composition of the depleted MORB mantle (DMM), *Earth Planet. Sci. Lett.*, *231*(1–2), 53–72.
Wright, T. J., C. Ebinger, J. Biggs, A. Ayele, G. Yirgu, D. Keir, and A. Stork (2006), Magma-maintained rift segmentation at continental rupture in the 2005 Afar dyking episode, *Nature*, *442*, 291–294.
Zellmer, G. F., K. H. Rubin, K. Grönvold, and Z. Jurado-Chichay (2008), On the recent bimodal magmatic processes and their rates in the Torfajökull-Veiðivötn area, Iceland, *Earth Planet. Sci. Lett.*, *269*(3–4), 388–398.